



Universiteit
Leiden
The Netherlands

Small molecule inhibitors of Nicotinamide N-Methyltransferase (NNMT)

Gao, Y.

Citation

Gao, Y. (2021, September 29). *Small molecule inhibitors of Nicotinamide N-Methyltransferase (NNMT)*. Retrieved from <https://hdl.handle.net/1887/3213827>

Version: Publisher's Version

License: [Licence agreement concerning inclusion of doctoral thesis in the Institutional Repository of the University of Leiden](#)

Downloaded from: <https://hdl.handle.net/1887/3213827>

Note: To cite this publication please use the final published version (if applicable).

Chapter 5

Bisubstrate inhibitors of nicotinamide *N*-methyltransferase bearing warheads for covalent interaction with cysteine and serine residues

Manuscript in preparation

Abstract

Nicotinamide *N*-methyltransferase (NNMT) catalyses the methylation of nicotinamide using the cofactor *S*-adenosyl-L-methionine (SAM) as a methyl donor. NNMT has been implicated in various diseases, including cancer and metabolic disorders. Therefore, potent, and selective NNMT inhibitors are valuable tools to study the biological functions and therapeutic potential of NNMT. Covalent inhibition is a rapidly growing discipline within drug discovery. Here, we describe our efforts to design covalent inhibitors targeting non-catalytic cysteine residues (C159 and C165) and serine residues (S201 and S213) involved in substrate binding in the NNMT active site. Acrylamides and chloroacetamides were used as warheads to target the cysteine residues and sulfonyl fluoride and boronic acid groups were used to target serine. After linker optimization, a chloroacetamide-containing inhibitor gave good inhibition of NNMT (compound **17b**, IC_{50} = 400 nM) and was found to be the first example of a potent NNMT bisubstrate type inhibitor lacking the amino acid motif present in SAM. The replacement of the aromatic nitrile in lead compound **17u** (chapter 3) with a sulfonyl fluoride at either the *meta*- or *para*-position gave potent inhibition of NNMT with IC_{50} values of 68-89 nM for compounds **39a** and **39b**. Modelling data predicts that the distance and orientation of the sulfonyl fluoride moieties may allow for covalent interaction with active site serine residues. Experiments to further characterize the mechanistic details of these inhibitors are currently ongoing.

1. Introduction

Nicotinamide *N*-methyltransferase (NNMT) is a key cytoplasmic enzyme in the human body, which is responsible for the methylation of the nicotinamide (NA), using *S*-adenosyl-*L*-methionine (SAM) as the methyl donor.^{1–3} The physiological function of NNMT is related to various human diseases in the past years. The main functions of NNMT were assumed to be linked to NA metabolism and xenobiotic detoxification of endogenous metabolites. However, the role that NNMT plays in human health and disease is becoming more apparent and seems to be much more complex.⁴ Overexpressed NNMT has been observed in various disorders, including cardiovascular disease,^{5,6} metabolic disorders,^{7–9} neurodegenerative disease,^{10,11} and cancer.^{12–16} It seems that NNMT has a role in regulating epigenetic modifications and signal transduction, making it a promising and valuable therapeutic target.^{17,18} Given the increased interest in NNMT as a potential therapeutic target, a variety of NNMT inhibitors have recently been disclosed, including SAM-competitive inhibitors, nicotinamide-competitive inhibitors, bisubstrate inhibitors, natural product inhibitors, peptides inhibitors, and covalent inhibitors.¹⁹ Generally speaking, covalent inhibitors have several potential advantages, including sustained duration of action, increased ligand efficiency, the ability to overcome endogenous ligands, optimized capability to avoid resistant mutations, and increased selectivity of some clinically isolated variants.²⁰

In this chapter, we aimed to expand upon the available set of bisubstrate NNMT inhibitors developed in our group (**chapters 2 and 3**) by the introduction of covalent warheads. The active site of NNMT contains several non-catalytic cysteine residues, specifically C159 and C165, which can be targeted for covalent modification. In addition, the NA substrate pocket of NNMT contains two important, but non-essential active site serine residues (S201 and S213) which are involved in the interaction of the amide moiety of NA. Mutation of these cysteine and serine residues to alanine does not impair the activity of the enzyme.^{21–23} Previous work by Cravatt and co-workers has also demonstrated the feasibility of covalent inhibition of NNMT.²² In their work, an activity-based protein profiling study was performed using probes based on *S*-adenosyl-*L*-homocysteine (SAH), the biproduct of the NNMT enzymatic methylation reaction, to profile methyltransferases in various human cancer cell lines (renal carcinoma 769P, ovarian cancer OVCAR3, and melanoma MUM2C). Subsequently, the SAH-probe was used as a fluorescence polarization (FP) probe to screen a set of electrophilic fragments identifying the first covalent NNMT inhibitor (RS004 (**1**), Figure 1) which displayed an IC₅₀ value of 10 μM. Through mutation of active site cysteine residue C165 to alanine, the compound was confirmed to covalently engage with this residue.²² The structure of RS004 was optimized through a structure-activity relationship (SAR) study, resulting in the more potent compounds HS58a (**2**) and HS312 (**3**) which showed

submicromolar IC_{50} values (Figure 1).²⁴ In an alternative approach, Sen et al. reported 4-chloropyridine analogs (**4-6**) as NNMT suicide substrates. Upon NNMT mediated *N*-methylation of the chlorinated substrates, the now positively charged pyridine ring enhances the electrophilicity of the C4 position, thereby facilitating an aromatic nucleophilic substitution by the non-catalytic C159 residue.²³ In a third approach, Resnick et al. described the high-throughput screening of ca. 1000 electrophilic fragments against cysteine-containing enzymes, identifying several fragments that covalently modified NNMT (compounds **7-9**).²⁵ However, when we evaluated these compounds using our in-house NNMT inhibition assay, none of them showed significant NNMT inhibition when tested at a concentration of 100 μ M (unpublished data).

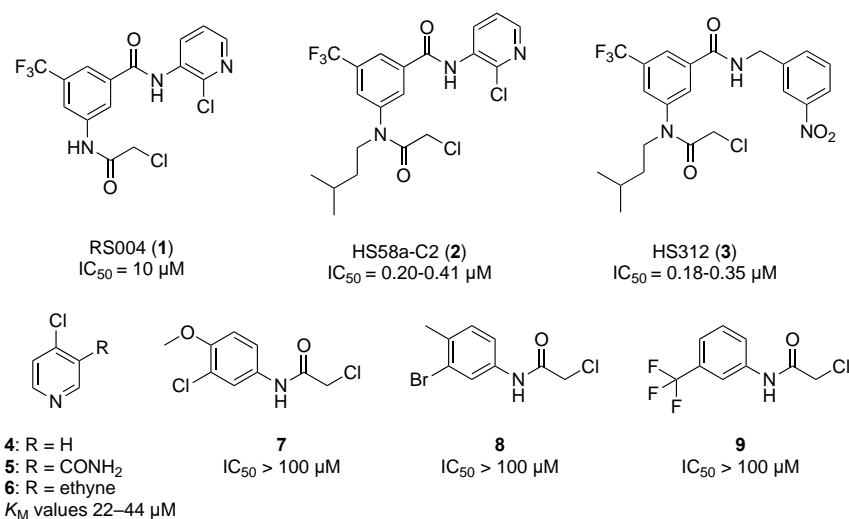


Figure 1. The structures of published covalent NNMT inhibitors featuring the chloroacetamide moiety as a warhead (compounds **1-3** and **7-9**). Compounds **4-6** are substrates which become covalent modifiers of an active site cysteine upon NNMT-mediated methylation.

Compound Design

The crystal structure of NNMT bound to its natural substrate NA and the product of the enzymatic reaction SAH (PDB ID: 3ROD) reveals multiple interactions with active site residues, including cysteine C165 that interacts with the ribose oxygen, and serine residues S201 and S213 that interact with the carbonyl of the NA substrate (Figure 2A).²¹ Notably, results of a modelling study performed with the very potent NNMT inhibitor **17u** (chapter 3) suggest that the nitrile group is interacting with two active site serine residues (S201 and S213, Figure 2B).

In an NMR-based activity assay Gilbert et al. measured the reactivity of various covalent warheads against serine and cysteine residues: the two most common residues targeted for covalent inhibition.²⁶ Building from this information, as well as from the structures of recently reported covalent NNMT inhibitors (Figure 1), we selected the acrylamide and chloroacetamide

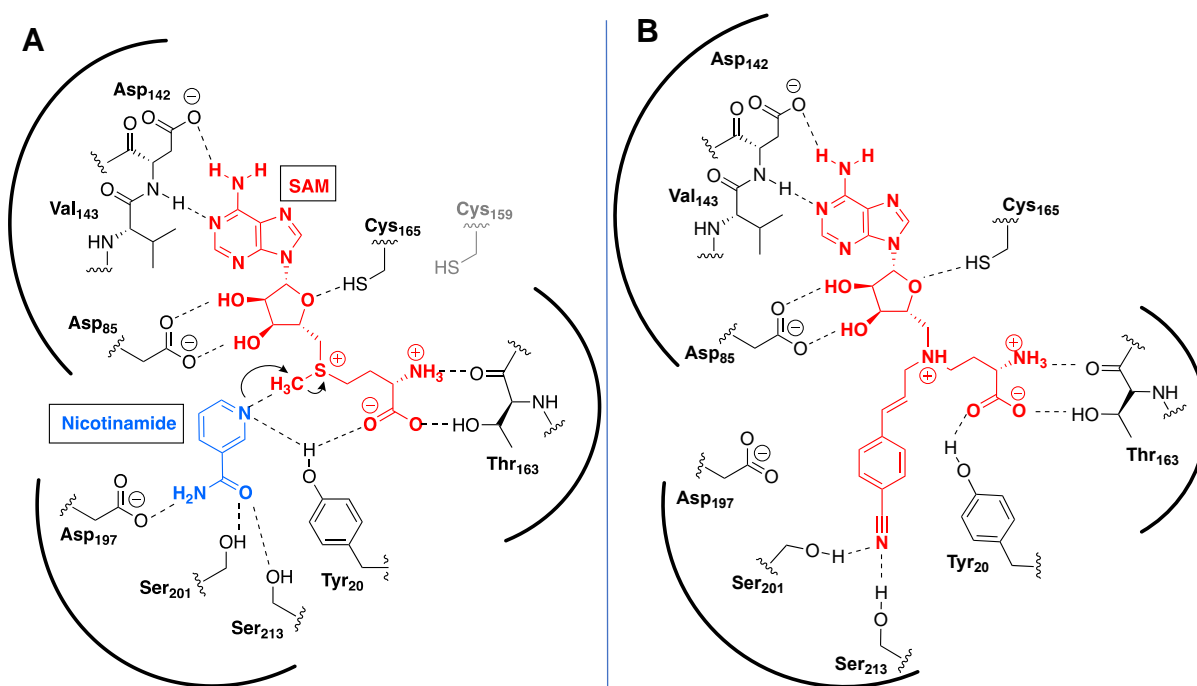


Figure 2. Schematic overview of the active site of NNMT. A) Interactions of active site residues with substrate NA and product SAH indicating the presence of cysteine residues C159 and C165 and serine residues S201 and S213. B) Compound **17u** (chapter 3) modelled in the active site of NNMT

moieties as Michael acceptor “warheads” in an attempt to target cysteine residues C159 and C165. In search of other warheads to covalently modifying serine residues S201 and S213, we selected the boronic acid and sulfonyl fluoride moieties. The boronic acid motif is found in a variety of clinically approved drugs, like Bortezomib, Tavaborole, and Vaborbactam, which have been approved for treatment of cancer and fungal infections, and bacterial infections.²⁷ The boric acids form a reversible covalent interaction with serine or threonine residues in their protein targets. The use of the sulfonyl fluoride moiety as a covalent warhead was first reported by Fahrney,²⁸ and was subsequently broadly investigated as a covalent warhead for protein modification. As a covalent warhead, sulfonyl fluorides show good reactivity towards active site serine residues and as such are often used in protease inhibitors. Furthermore, sulfonyl fluorides are known to interact with threonine, lysine, tyrosine, cysteine and histidine residues.²⁹ This feature may help in identifying other residues in NNMT that can be targeted for covalent inhibition.

Based on the structural and modelling data available, our design of covalent bisubstrate NNMT inhibitors focussed on the introduction of the acrylamide and chloroacetamide moieties in place of the amino acid functionality as well as the introduction of boronic acid and sulfonyl fluoride warheads on the aromatic ring in the substrate pocket (Figure 3). The Michael acceptors

were incorporated with a variety of linkers to probe the optimal length and rigidity for the position of the warheads. The warheads on the aromatic ring were investigated at both the meta and para-position. as both para-cyano and meta-amide lead compounds **17u** and **17v** (Figure 3) showed potent inhibition of NNMT and are predicted to interact with serine residues S201 and S213.

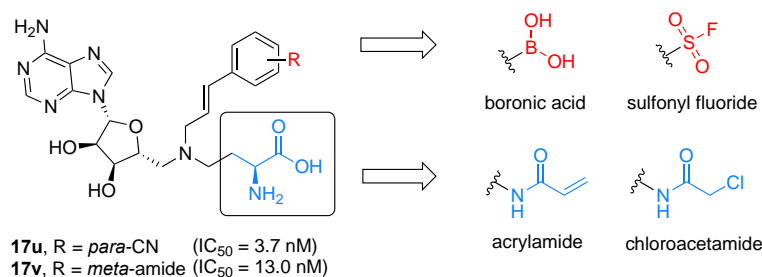
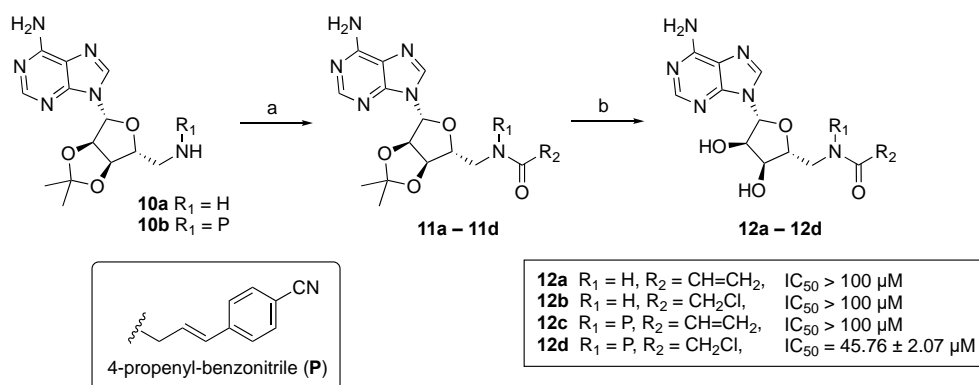


Figure 3. The design of the covalent NNMT inhibitors was based on the structure of lead compounds **17u** and **17v**, which were modified to target active site serine residues with boronic acids and sulfonyl fluoride motifs (red) or modified with acrylamide and chloroacetamide motifs to target active site cysteine residues.

Synthesis of cysteine targeting compounds

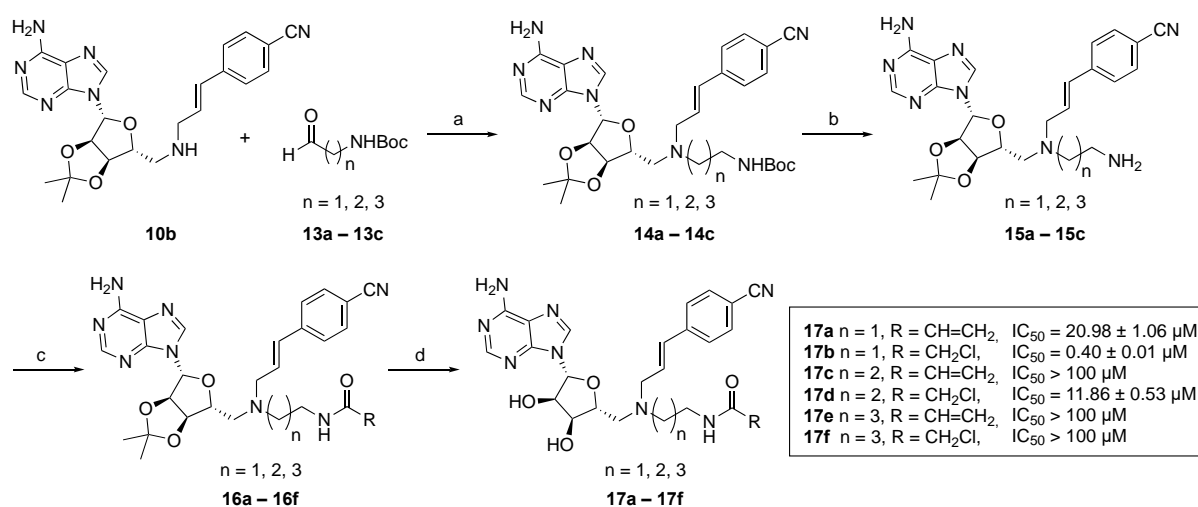
Using our modular double reductive amination procedure, we first prepared compounds **12a-d** to investigate the role of the aromatic sidechain and the choice of warhead. In this route, 5'-amino-5'-deoxy-2',3'-O-isopropylideneadenosine **10a** or the propenyl-4-cyanophenyl linked compound **10b** was treated with acryloyl chloride or chloroacetyl chloride to obtain intermediates **11a-d** which were subsequently deprotected using TFA and purified by preparative HPLC to give final compounds **12a-d** (Scheme 1). Unfortunately, compounds **12a-c** did not show any measurable activity against NNMT and compound **12d** showed only poor inhibition with an IC_{50} of $45.76 \pm 2.07 \mu\text{M}$. These findings hinted at the importance of the aromatic sidechain and the



Scheme 1. Synthetic Route for compounds **12a – 12d**. Reagents and conditions: (a) acryloyl chloride or chloroacetyl chloride, DIPEA, DCM, 2h; (b) TFA, DCM, H_2O , rt, 2h (two steps, 18 – 38%).

need to optimize the spacing of the warhead.

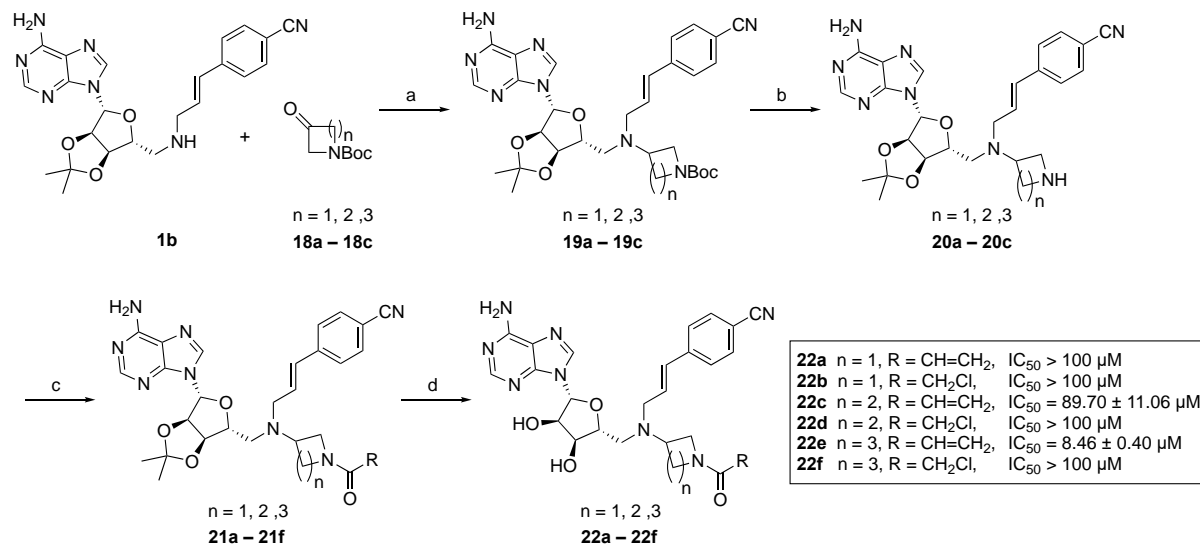
We then prepared compounds **17a-17f** (Scheme 2), in which the propenyl-4-cyanophenyl was maintained and the linker between the central nitrogen and the warhead was varied from 2 to 4 carbons. Starting from compound **1b**, aldehydes **13a-c** were coupled to offer intermediates **14a-c**. Next, the Boc-group was removed selectively using water-free acidic conditions and the corresponding amines **15a-c** coupled with acryloyl chloride or chloroacetyl chloride. Finally, the isopropylidene group was cleaved using aqueous acidic conditions and the crude products were purified to yield compounds **17a-f**. For acrylamide **17a** only moderate activity was observed ($IC_{50} = 20.98 \pm 1.06 \mu M$) while compounds **17c** and **17e** bearing longer spacers, showed no inhibition of NNMT. The chloroacetamides, however, showed more promising results with increasing activity with decreasing spacer length. While no activity was observed for compound **17f**, compound **17d** exhibited moderate activity ($IC_{50} = 11.86 \pm 0.53 \mu M$), which was further improved in the case of compound **17b**, which exhibits sub-micromolar inhibition of NNMT ($IC_{50} = 0.40 \pm 0.01 \mu M$). Notably, this is the first example of a bisubstrate inhibitor of NNMT in which the amino acid functionality is replaced by a less polar functionality while retaining significant activity.



Scheme 2. Synthetic route for compounds **17a – 17f**. Reagents and conditions: (a) $NaBH(OAc)_3$, DCE, AcOH (65-72% yield); (b) TFA, dry DCM; (c) acryloyl chloride or chloroacetyl chloride, DIPEA, DCM (d) TFA, DCM, H_2O , rt. 2h (18-47% yield, 3 steps).

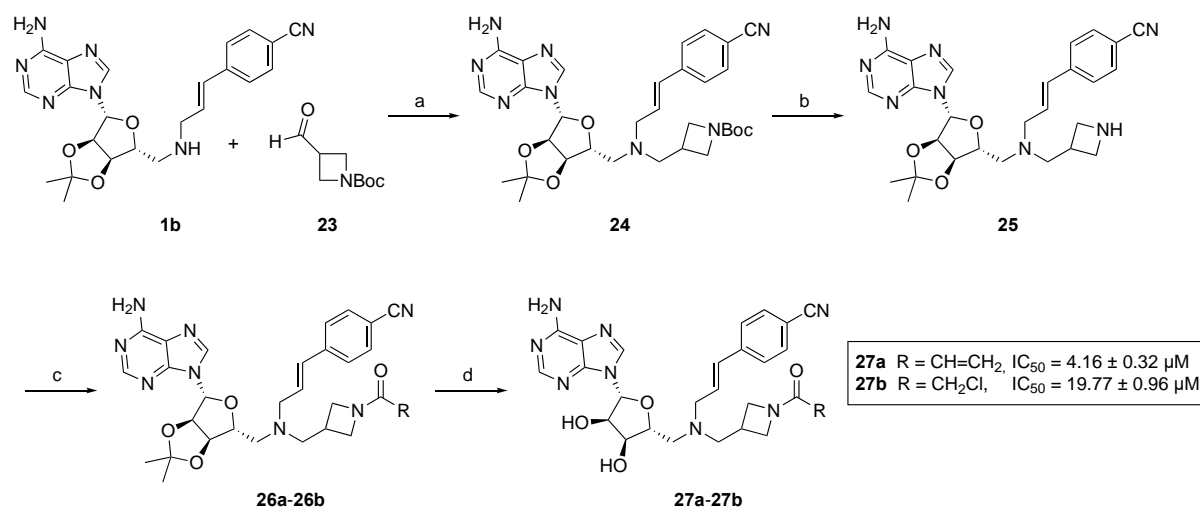
Building on the promising results obtained with compound **17b**, we next focussed on the further optimization of the linker. Instead of the linear linkers, we investigated a series of 4-, 5- or 6-membered cyclic linkers (Scheme 3 and 4). To synthesize these compounds, amine **1b** was subjected to reductive amination with ketones **18a-c** (Scheme 3) or aldehyde **23** (Scheme 4). As

before, the Boc group was then selectively deprotected and the resulting amine coupled to acryloyl chloride or chloroacetyl chloride to form intermediates **21a-f** and **26a-b** which were then deprotected and purified to give final compounds **22a-f** and **27a-b**. For the chloroacetamide-containing compounds, no improvement in activity was found with the best results found for compound **27b** ($IC_{50} = 19.77 \pm 0.96 \mu M$). For the acrylamides however, compounds **22e** ($IC_{50} = 8.46 \pm 0.40 \mu M$), and **27a** ($IC_{50} = 4.16 \pm 0.32 \mu M$), now showed low micromolar inhibition.



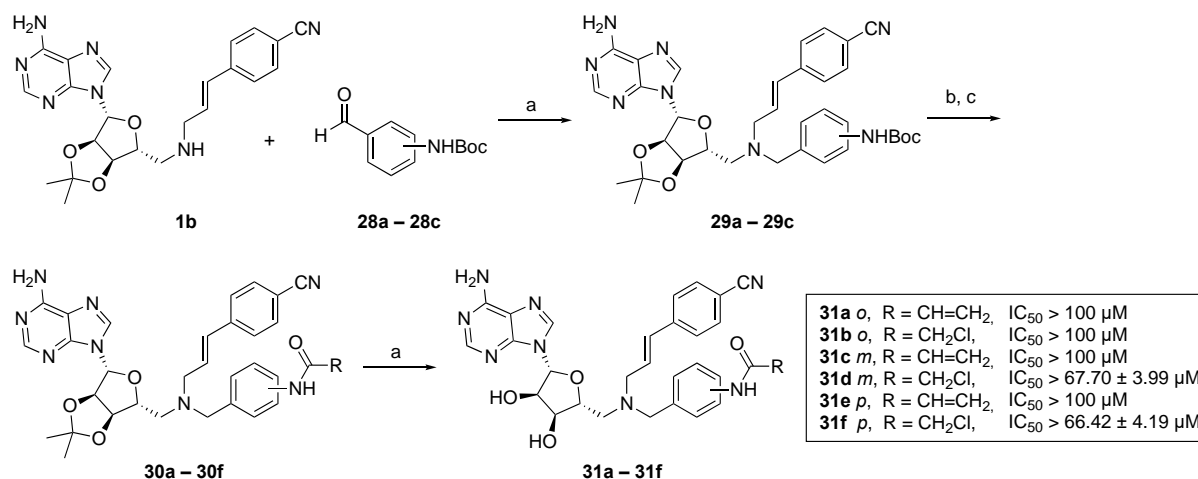
Scheme 3. Synthetic route for compounds **22a – 22f**. Reagents and conditions: (a) $NaBH(OAc)_3$, DCE, AcOH (17–63% yield); (b) TFA, dry DCM; (c) acryloyl chloride or chloroacetyl chloride, DIPEA, DCM (d) TFA, DCM, H_2O , rt. 2h (23–39% yield, 3 steps).

To investigate aromatic linkers, a benzyl-based moiety was introduced bearing the



Scheme 4. Synthetic route for compounds **27a – 27b**. Reagents and conditions: (a) $NaBH(OAc)_3$, DCE, AcOH, (35%); (b) TFA, dry DCM; (c) acryloyl chloride or chloroacetyl chloride, DIPEA, DCM (d) TFA, DCM, H_2O , rt. 2h (20–28%, over 3 steps).

acrylamide or chloroacetamide warhead at the *ortho*, *meta* or *para* position (Scheme 5). To this end, compound **1b** was coupled with *tert*-butyl 4-formylphenylcarbamates **28a-c**. As before, the Boc group was selectively deprotected and the resulting anilines **29a-c** coupled to acryloyl chloride or chloroacetyl chloride to form intermediates **30a-f**. Final deprotection and purification gave compounds **31a-f**. Unfortunately, the introduction of the aromatic ring did not improve the activity of the compounds.

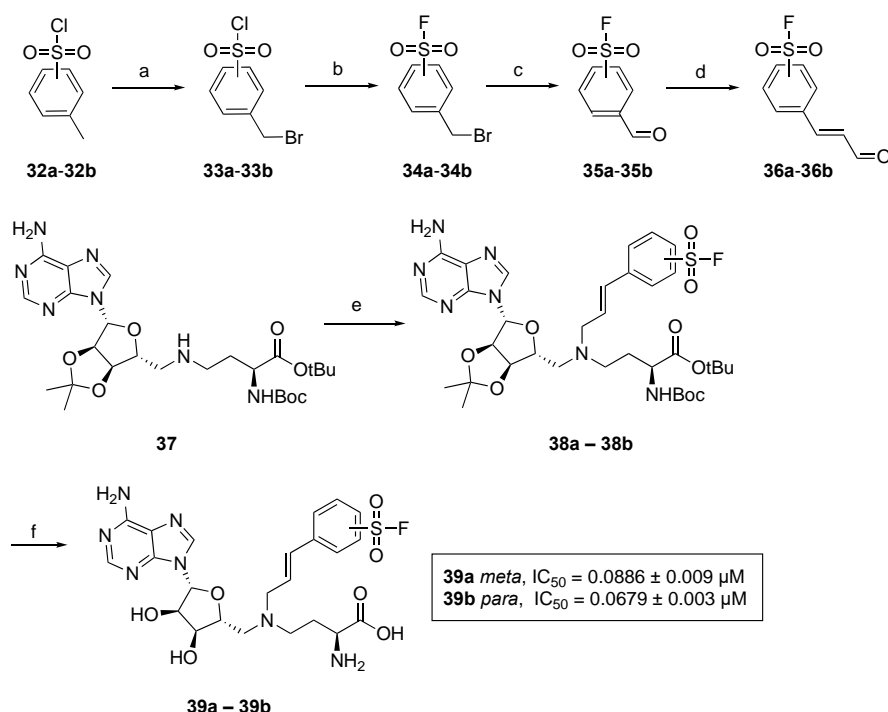


Scheme 5. Synthetic route for compounds **31a – 31f**. Reagents and conditions: (a) NaBH(OAc)₃, DCE, AcOH (21 – 56% yield); (b) TFA, dry DCM; (c) acryloyl chloride or chloroacetyl chloride, DIPEA, DCM (d) TFA, DCM, H₂O, rt. 2h (22-41% yield, 3 steps).

As noted above, in our attempts to develop covalent bisubstrate NNMT inhibitors, compound **17b** was identified as the most potent compound and bears the chloroacetamide moiety in place of the amino acid functionality. Ongoing work is focussing on establishing the proposed covalent mechanism of this inhibitor both by whole protein mass spectrometry to analyse the formation of the enzyme-inhibitor adduct as well as biochemical assays using enzyme mutants in which one or more of the target cysteine residues is mutated to an alanine. For these experiments we recently obtained the C159A, C165A and C159A/C165A mutants, all of which are catalytically still active. Should a covalent interaction with either of these cysteine residues play a covalent role in the activity of **17b**, the activity of the inhibitor would be expected to be reduced against the mutant enzyme.

Synthesis of serine targeting compounds

For the serine-targeting compounds containing the sulfonyl fluoride warheads, commercially available methylbenzenesulfonyl chlorides **32a-b** were brominated with benzoyl peroxide (BPO) and *N*-bromo-succinimide to form bromomethylbenzenesulfonyl chlorides **33a-b** and subsequently converted to the corresponding sulfonyl fluorides **34a-b** using hydrogen fluoride (Scheme 6). Compounds **34a-b** were then oxidized directly using *N*-methylmorpholine *N*-oxide (NMO) in the presence of 4Å molsieves to offer the corresponding aldehydes **35a-b** which were extended via a Wittig reaction to obtain cinnamic aldehydes **36a-b**. The aldehydes were coupled with amine **37** via a reductive amination reaction to obtain intermediates **38a-b** and after deprotection using TFA and purification by preparative HPLC, final compounds **39a-b** were obtained.

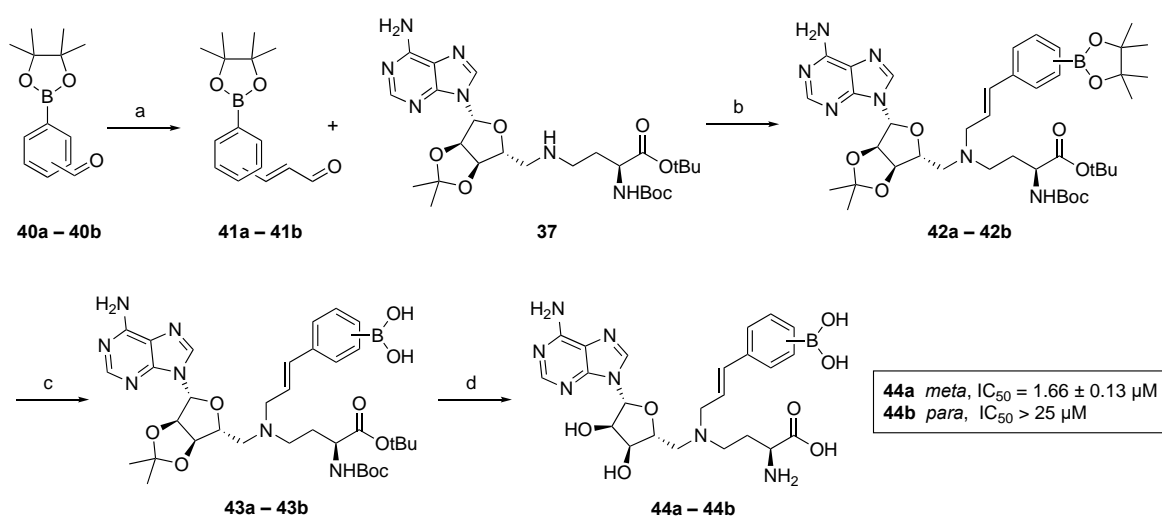


Scheme 6. Synthetic route for compounds **39a** – **39b**. Reagent and conditions: (a) Benzoyl peroxide, *N*-bromosuccinimide, ACN, reflux (8-25%); (b) HF.KF, H₂O/ACN, rt, (31-80%); (c) *N*-methylmorpholine *N*-oxide, 4Å molsives, ACN, rt (50-75%); (d) PPh₃=CHCHO, THF, 50°C, overnight (44 – 67%); (e) **36a** or **36b**, NaBH(OAc)₃, DCE, AcOH (67% – 71%); (f) TFA, DCM, H₂O, rt, 2h (71– 82%).

When evaluating the sulfonyl fluoride compounds, we found that incorporation of the sulfonyl fluoride at either the *meta*- and *para*-position relative to the alkene linker, both resulted in potent inhibition of NNMT with IC₅₀ values of 89 and 68 nM respectively. Until now, the position on the aromatic ring at which a substitution was incorporated had a significant impact

into its activity. However, for compounds **39a** and **39b**, no significant difference is observed. Experiments are ongoing to establish the mode of action of these inhibitors. Specifically, looking into the covalent nature of the mechanism through whole protein MS and biochemical assays. For these experiments we have obtained the single and double serine-to-alanine mutants (S201A, S213A, S201A/S213A), all of which are catalytically still active. Should a covalent interaction with either of these serine residues play a role in the mechanism of action for **39a** or **39b**, the activity of the compound(s) will likely be significantly impacted against NNMT mutants wherein these serine residues are exchanged for alanine.

For the synthesis of the boronic acid containing compounds, we started from pinacolatoboron aldehydes **40a-b** which were extended via Wittig reaction to obtain cinnamic aldehydes **41** (Scheme 7). The aldehydes were subsequently coupled with amine **37** to offer compounds **42a-b**. The pinacol protecting groups were cleaved under oxidative conditions using NaIO₄ yielding compounds **43a-b**. Final compounds **44a-b** were obtained by global deprotection of the acid-labile protecting groups using TFA.



Scheme 7. Synthetic route for compounds **44a – 44b**. Reagent and conditions: (a) PPh₃=CHCHO, THF, 50 °C, overnight (15 – 36%); (b) NaBH(OAc)₃, DCE, AcOH (37 – 44%); (c) NaIO₄, 0.2 M HCl(aq), THF, 2h; (d) TFA, DCM, H₂O, rt, 2h (17 – 38%, over two steps).

The analysis of boronic acid substituted compounds **44a-b** revealed a steep SAR with no appreciable inhibition observed for para-substituted boronic acid **44b**, but low micromolar inhibition seen for meta-substituted boronic acid **44a** (IC₅₀ value of 1.66 ± 0.13 μM). This is the same trend as observed for the amide substituted compounds (**chapter 3**), which could suggest that the boronic acids are mimicking the amide functional group, only less efficiently. To evaluate

the mode of action of the boronic acid analogues, the compounds will be evaluated in biochemical assays using the serine-to-alanine mutants of NNMT as described above.

Modelling Studies

To further explore how the inhibitors described in this chapter might bind within the NNMT active site, docking studies were carried out using Autodock Vina³⁰. Using available crystal structures of NNMT bound to previously reported bisubstrate inhibitor LL320 (PDB ID: 6PVS),³¹ compounds **17b**, **39a-b**, and **44a-b** were docked in the NNMT active site. Overlaying compound **17b** with the ligand LL320 show good overlay, but no hydrogen bonding interactions are predicted for the chloroacetamide moiety binding in the amino acid pocket. In addition, it seems that the covalent warhead of compound **17b** does not have the correct spacing and orientation to engage with cysteine residues C159 or C165 in the NNMT active site. The distance between the α -carbon of the chloroacetamide and the sulphur atom of C165 is around 8.2 Å in the overlay and cysteine C159 is located even further away. These distances would be too large to be able to form a covalent interaction (Figure 4). Nevertheless, compound **17b** still shows good NNMT inhibition, which indicates that the chloroacetamide warhead is well accommodated in the active site, e.g. through hydrophobic interactions.

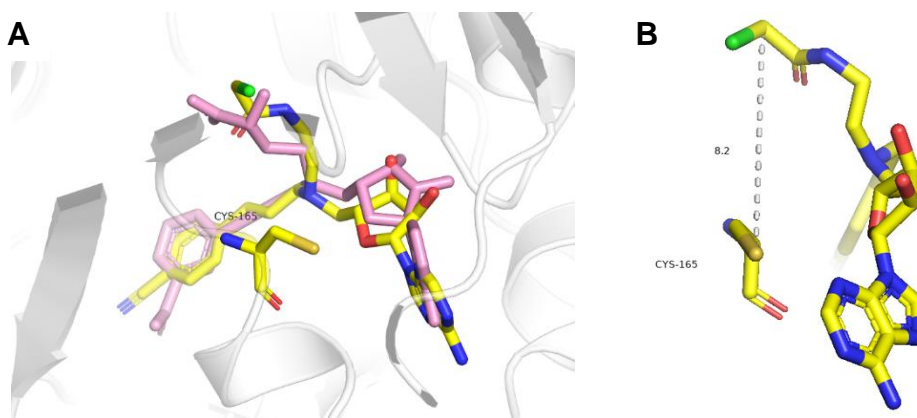


Figure 4. (A) Overlay of the docking model of compound **17b** with the crystal structure of compound LL320 (pink) bound to hNNMT (gray), and (B) the distance between the α -carbon of the chloroacetamide in **17b** to the sulphur atom of cysteine residue C165 is around 8.2 Å, which would be too far to form a covalent interaction.

Compounds **39a**, **39b**, **44a**, and **44b** were designed to covalently target serine residues S201 or S213. Therefore, the focus of modelling these compounds was on the interactions of the

sulfonyl fluoride and boronic acid substitutions with the serine residues in the nicotinamide pocket of NNMT. When docking compounds **39a-b** in the NNMT active site (PDB ID: 6PVS), good overlay with compound LL320 was found (Figure 5A) and both the *meta*- and *para*-substituted sulfonyl fluorides appear to be close enough to serine residues S201 and S213 to possible engage in covalent interactions with predicted distances of 2.9 and 3.4 Å respectively (Figure 6A and 6B). The docking of both *meta*- and *para*-substituted boronic acid compounds **44a-b** revealed a slight difference in overlay with compound LL320 for *para*-substituted boronic acid compound **44b** while the *meta*-substituted boronic acid compound **44a** showed a similar orientation of the boronic acid motif with the amide moiety of LL320 (Figure 5B). This may explain the difference in activity observed for **44a** and **44b**. However, from the modelling data of compounds **44a** and **44b**, no clear explanation for the difference in activity can be found as in both cases the boronic acid seems to be in close proximity with both targeted serine residues (Figure 6C and 6D).

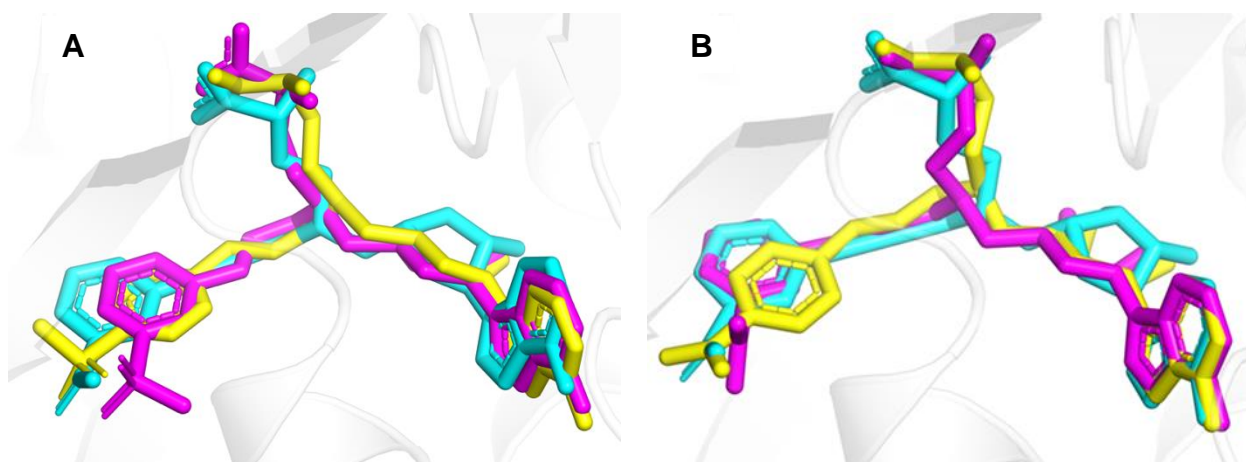


Figure 5. A) Overlay of the docking models of compounds **39a** (pink) and **39b** (yellow) with the hNNMT (gray)–LL320 (cyan) complex (PDB 6PVS), (B) Overlay of the docking models of compounds **44a** (pink) and **44b** (yellow) with the hNNMT (gray)–LL320 (cyan) complex (PDB 6PVS).

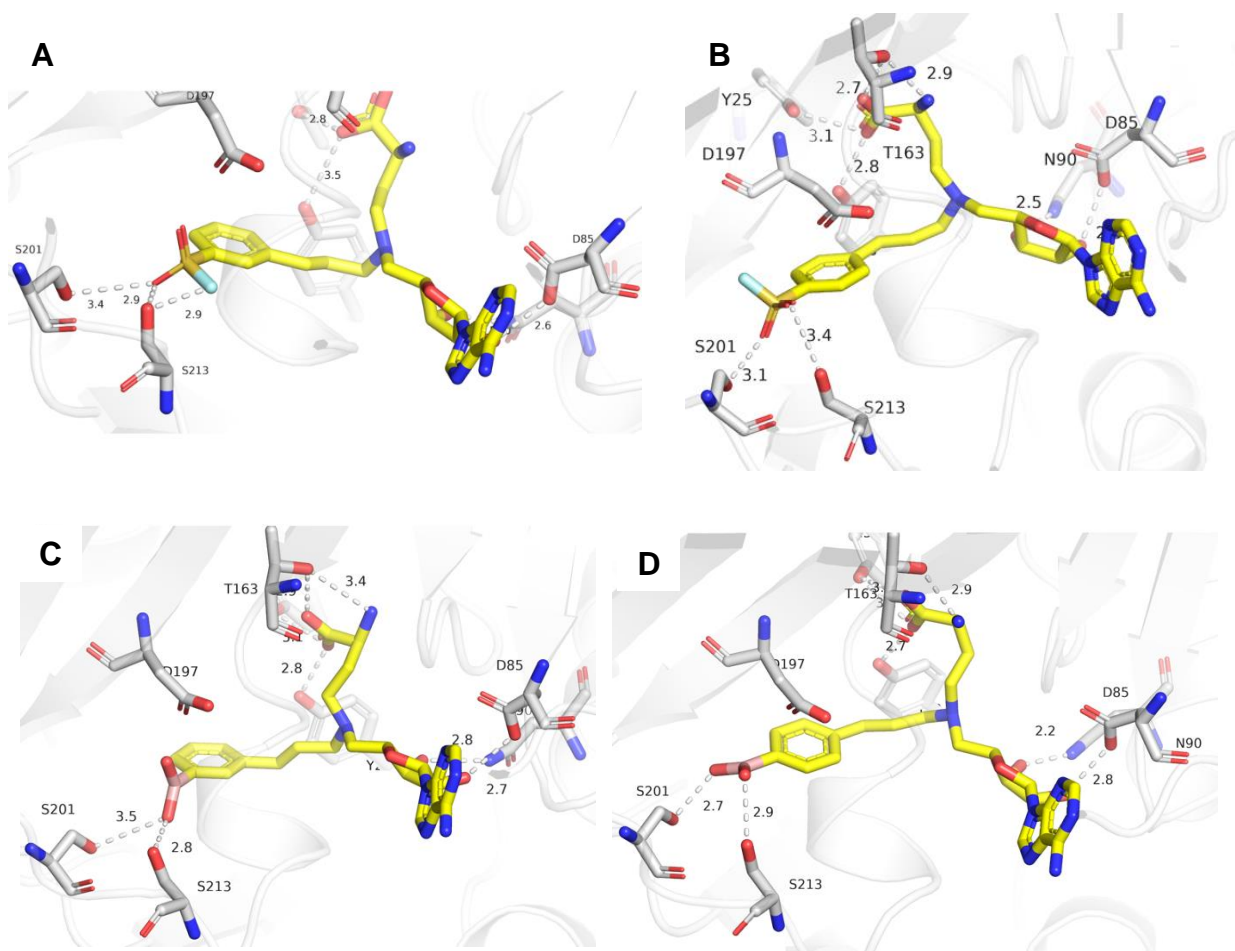


Figure 6. Docking analysis of compounds **39a** (A), **39b** (B), **44a** (C) and **44b** (D) in the binding sites of hNNMT (gray) structure (PDB ID: 6PVS). Hydrogen bonding interactions are shown in gray dotted lines with calculated distances in Angstrom.

Conclusions

Building on the structure of the potent bisubstrate NNMT inhibitors **17u** and **17v**, described in **chapter 3**, we designed and synthesized a focused library of novel inhibitors containing different warheads designed to target cysteine or serine residues in the NNMT active site. To this end, the amino acid functionality was replaced by acrylamides and chloroacetamides with different linkers and evaluated for their inhibitory activity of NNMT with the aim of interacting with cysteine residues C159 or C165, previously targeted by covalent inhibitors of NNMT. In addition, serine residues S201 and S213, involved in binding to the amide moiety of NA pocket, were targeted using sulfonyl fluoride and boronic acid groups. By probing the NNMT binding pockets with different linkers and covalent warheads, we found that linker length is crucial for activity. Among the Michael-acceptor compounds prepared, compound **17b** showed the most potent activity with

an IC₅₀ value of 400 nM. It is noteworthy to mention, that this is the first example of a bisubstrate inhibitor of NNMT in which the amino acid functionality is replaced whilst partially retaining its activity. Whether or not the interaction of compound **17b** with the NNMT active site is covalent is still under investigation.

In pursuit of targeting the serine residues in the nicotinamide pocket of NNMT, sulfonyl fluoride analogues **39a** and **39b** showed very promising activity with both compounds exhibiting nanomolar activity. As described in **chapter 3**, we previously found that the orientation of electron withdrawing functional groups at the aromatic ring generally have a preference for the *para*-position and only the amide functionality was found to be most active in the *meta*-position. In the case of the sulfonyl fluoride motif, both orientations work equally well. Modelling of compounds **39a-b** indicate that the sulfonyl fluoride moiety in both compounds is in close proximity to serine residues S201 and S213, potentially allowing for a covalent interaction. For the boronic acid derivatives, only *meta*-orientated boronic acid compound **44a** showed activity, albeit with a moderate IC₅₀ value of 1.6 μM. Compound **44b**, which has its boronic acid motif in the *para*-position, did not show any activity. No clear explanations can be provided for the potencies of compounds **44a-b** based on the modelling data obtained. The role of the serine residues is currently under investigation involving the use serine-to-alanine mutants of NNMT.

Experimental Procedures

General Procedures

All reagents employed were of American Chemical Society grade or finer and were used without further purification unless otherwise stated. For compound characterization, ¹H NMR spectra were recorded at 400 MHz or 500MHz with chemical shifts reported in parts per million downfield relative to tetramethylsilane, H₂O (δ 4.79), CHCl₃ (7.26), or methanol (δ 3.31). ¹H NMR data are reported in the following order: multiplicity (s, singlet; d, doublet; t, triplet; q, quartet; and m, multiplet), coupling constant (*J*) in hertz (Hz) and the number of protons. Where appropriate, the multiplicity is preceded by br, indicating that the signal was broad. ¹³C NMR spectra were recorded at 101 MHz with chemical shifts reported relative to CDCl₃ (δ 77.16), methanol (δ 49.00), or DMSO (δ 39.52). The ¹³C NMR spectra of the compounds recorded in D₂O could not be referenced. High-resolution mass spectrometry (HRMS) analysis was performed using a Q-TOF instrument. Compounds **1b**, **4a**,³² **4b**,³³ **4c**,³⁴ **34a**,³⁵ **34b**³⁶ and **37**, were prepared as previously described and had NMR spectra and mass spectra consistent with the assigned structures.

N-(((3*aR*,4*R*,6*R*,6*aR*)-6-(6-amino-9*H*-purin-9-yl)-2,2-dimethyltetrahydrofuro[3,4-d][1,3]dioxol-4-yl)methyl)acrylamide (**11a**). To a solution of 9-(((3*aR*,4*R*,6*R*,6*aR*)-6-(aminomethyl)-2-methyltetrahydrofuro[3,4-d][1,3]dioxol-4-yl)-9*H*-purin-6-amine **10a** (10 mg, 0.033 mmol) in 5 mL DMF were added 0.1 mL DIPEA and 0.1 mL acryloyl chloride under ice bath. After the addition, the ice bath was removed the mixture stirred at rt 2 hours, then removed the solvent under reduced pressure and the residue (yellow oil) **11a** was not purified for next step.

N-(((3*aR*,4*R*,6*R*,6*aR*)-6-(6-amino-9*H*-purin-9-yl)-2,2-dimethyltetrahydrofuro[3,4-d][1,3]dioxol-4-yl)methyl)-2-chloroacetamide (**11b**) Following the procedure described for compound **11a**, coupling **10a** (10 mg, 0.033 mmol) and 2-chloroacetyl chloride (0.1 mL) afforded compound **11b** as yellow oil without purification for next step.

N-(((3*aR*,4*R*,6*R*,6*aR*)-6-(6-amino-9*H*-purin-9-yl)-2,2-dimethyltetrahydrofuro[3,4-d][1,3]dioxol-4-yl)methyl)-*N*-((*E*)-3-(4-cyanophenyl)allyl)acrylamide (**11c**). Following the procedure described for compound **11a**, coupling 4-((*E*)-3-(((3*aR*,4*R*,6*R*,6*aR*)-6-(6-amino-9*H*-purin-9-yl)-2,2-dimethyltetrahydrofuro[3,4-d][1,3]dioxol-4-yl)methyl)amino)prop-1-en-1-yl)benzonitrile **10b** (15 mg, 0.033 mmol) and acryloyl chloride (0.1 mL) afforded compound **11c** as yellow oil without purification for next step.

N-(((3*aR*,4*R*,6*R*,6*aR*)-6-(6-amino-9*H*-purin-9-yl)-2,2-dimethyltetrahydrofuro[3,4-d][1,3]dioxol-4-yl)methyl)-2-chloro-*N*-((*E*)-3-(4-cyanophenyl)allyl)acetamide (**11d**). Following the procedure described for compound **11a**, compound **10b** (15 mg, 0.033 mmol) and 2-chloroacetyl chloride (0.1 mL) afforded compound **11d** as yellow oil without purification for next step.

N-(((2*R*,3*S*,4*R*,5*R*)-5-(6-amino-9*H*-purin-9-yl)-3,4-dihydroxytetrahydrofuran-2-yl)methyl)acrylamide (**12a**). To a solution of compound **11a** (14mg, crude) in 1 mL of CH₂Cl₂ has added a mixture of 9 mL TFA and 1 mL H₂O, and the solution was stirred for 2 h at room temperature. The mixture was concentrated, and the crude product was purified by preparative HPLC, affording compound **12a** as a yellow oil (4 mg, 38% yield over two steps, >70 % pure), LRMS (ESI): calculated for C₁₃H₁₇N₆O₄ [M+H]⁺ 321.13, found 321.16.

N-(((2*R*,3*S*,4*R*,5*R*)-5-(6-amino-9*H*-purin-9-yl)-3,4-dihydroxytetrahydrofuran-2-yl)methyl)-2-chloroacetamide (**12b**). Following the procedure described for compound **12a**, compound **11b** (16mg, crude) was deprotected and purified, affording compound **8** as a yellow powder (3 mg, 27% yield over two steps, > 70% pure). LRMS (ESI): calculated for C₁₂H₁₆ClN₆O₄ [M+H]⁺ 343.09, found 349.11.

N-(((2*R*,3*S*,4*R*,5*R*)-5-(6-amino-9*H*-purin-9-yl)-3,4-dihydroxytetrahydrofuran-2-yl)methyl)-*N*-((*E*)-3-(4-cyanophenyl)allyl)acrylamide (**12c**). Following the procedure described for compound **12a**, compound **11c** (21mg, crude) was deprotected and purified, affording compound **12c** as a white powder (5 mg, 32% yield over two steps, > 70% pure). LRMS (ESI): calculated for C₂₃H₂₄N₇O₄ [M+H]⁺ 462.1890, found 462.1892.

N-(((2*R*,3*S*,4*R*,5*R*)-5-(6-amino-9*H*-purin-9-yl)-3,4-dihydroxytetrahydrofuran-2-yl)methyl)-2-chloro-*N*-((*E*)-3-(4-cyanophenyl)allyl)acetamide (**12d**). Following the procedure described for compound **12a**, compound **11d** (25mg, crude) was deprotected and purified, affording compound **12d** as a yellow powder (3 mg, 18% yield over two steps, 70% pure). LRMS (ESI): calculated for C₂₂H₂₃ClN₇O₄ [M+H]⁺ 484.15, found 484.19.

tert-butyl (2-((((3*aR*,4*R*,6*R*,6*aR*)-6-(6-amino-9*H*-purin-9-yl)-2,2-dimethyltetrahydrofuro[3,4-*d*][1,3]dioxol-4-yl)methyl)((*E*)-3-(4-cyanophenyl)allyl)amino)ethyl)carbamate (**14a**). Amine **10b** (840 mg, 1.89 mmol), *tert*-butyl (2-oxoethyl)carbamate **13a** (360 mg, 2.26mmol), NaBH(OAc)₃ (600 g, 2.83 mmol) and AcOH (1 drop) were added to 1,2-dichloroethane (DCE, 50 mL) in a 250 mL round-bottom flask (RBF) and the mixture was stirred at room temperature under N₂ atmosphere overnight. The reaction was quenched by adding 1 N NaOH (20 mL), and the product was extracted with CH₂Cl₂. The combined organic layers were washed with brine and dried over Na₂SO₄. The solvent was evaporated, and the crude product was purified by column chromatography (5% MeOH in EtOAc) to give compound **14a** as a white powder (724 mg, 65% yield). ¹H NMR (400 MHz, CDCl₃) δ 8.17 (s, 1H), 7.88 (s, 1H), 7.49 (d, *J* = 8.3 Hz, 2H), 7.27 (d, *J* = 7.2 Hz, 2H), 6.63 (s, 2H), 6.39 (br d, *J* = 15.9 Hz, 1H), 6.28 – 6.18 (m, 1H), 6.03 (d, *J* = 1.9 Hz, 1H), 5.44 – 5.33 (m, 2H), 5.04 – 4.97 (m, 1H), 4.27 (q, *J* = 6.5 Hz, 1H), 3.26 (d, *J* = 6.0 Hz, 2H), 3.21 – 3.01 (m, 2H), 2.76 (d, *J* = 6.2 Hz, 2H), 2.59 (d, *J* = 5.2 Hz, 2H), 1.57 (s, 3H), 1.37 (br d, *J* = 12.7 Hz, 12H). ¹³C NMR (101 MHz, CDCl₃) δ 156.0, 153.0, 149.0, 141.3, 132.4, 131.1, 126.7, 120.2, 119.0, 114.6,

110.6, 90.4, 85.6, 83.9, 83.1, 56.8, 55.9, 53.7, 38.3, 28.5, 27.2, 25.5. HRMS (ESI): calculated for $C_{30}H_{39}N_8O_5$ $[M+H]^+$ 590.3043, found 590.3045.

tert-butyl 3-((((3*aR*,4*R*,6*R*,6*aR*)-6-(6-amino-9*H*-purin-9-yl)-2,2-dimethyltetrahydrofuro[3,4-*d*][1,3]dioxol-4-yl)methyl)((*E*)-3-(4-cyanophenyl)allyl)amino)pyrrolidine-1-carboxylate (**14b**). Following the procedure described for compound **14a**, compound **10b** (210 mg, 0.47 mmol) coupled with (9*H*-fluoren-9-yl)methyl (3-oxopropyl)carbamate **13b** (121 mg, 0.70 mmol) afforded compound **14b** as yellow powder (204 mg, 72% yield). 1H NMR (400 MHz, $CDCl_3$) δ 8.16 (s, 1H), 7.93 (s, 1H), 7.46 (d, J = 8.3 Hz, 2H), 7.23 (d, J = 8.3 Hz, 2H), 6.76 (s, 2H), 6.35 (br d, J = 16.0 Hz, 1H), 6.27 – 6.16 (m, 1H), 6.08 – 6.02 (m, 1H), 5.52 – 5.36 (m, 2H), 4.99 (dd, J = 5.6, 3.3 Hz, 1H), 4.36 – 4.32 (m, 1H), 3.25 – 3.00 (m, 4H), 2.68 (d, J = 6.8 Hz, 2H), 2.49 (t, J = 6.4 Hz, 2H), 1.56 (s, 3H), 1.35 (d, J = 7.2 Hz, 12H). ^{13}C NMR (101 MHz, $CDCl_3$) δ 156.0, 153.0, 149.0, 141.3, 139.5, 132.3, 131.2, 130.8, 126.6, 120.2, 119.0, 114.3, 110.4, 90.7, 85.8, 84.0, 83.3, 56.4, 51.8, 38.7, 28.5, 27.1, 25.4. HRMS (ESI): calculated for $C_{31}H_{41}N_8O_5$ $[M+H]^+$ 605.3200, found 605.3201.

tert-butyl (4-((((3*aR*,4*R*,6*R*,6*aR*)-6-(6-amino-9*H*-purin-9-yl)-2,2-dimethyltetrahydrofuro[3,4-*d*][1,3]dioxol-4-yl)methyl)((*E*)-3-(4-cyanophenyl)allyl)amino)butyl)carbamate (**14c**). Following the procedure described for compound **14a**, compound **10b** (210 mg, 0.47 mmol) coupled with *tert*-butyl (4-oxobutyl)carbamate **14** (130 mg, 0.70 mmol) afforded compound **5c** as yellow powder (200 mg, 69% yield). 1H NMR (400 MHz, $CDCl_3$) δ 8.22 (s, 1H), 7.95 (s, 1H), 7.50 (d, J = 8.3 Hz, 2H), 7.28 (d, J = 9.3 Hz, 2H), 6.53 (s, 2H), 6.38 (br d, J = 16.0 Hz, 1H), 6.31 – 6.22 (m, 1H), 6.06 (s, 1H), 5.49 – 5.43 (m, 1H), 4.97 (dd, J = 6.0, 3.3 Hz, 2H), 4.36 (s, 1H), 3.58 (s, 1H), 3.30 – 3.20 (m, 2H), 3.11 – 2.95 (m, 2H), 2.72 (d, J = 6.5 Hz, 2H), 2.48 (s, 2H), 1.57 (s, 3H), 1.38 (d, J = 13.7 Hz, 17). ^{13}C NMR (101 MHz, $CDCl_3$) δ 155.8, 153.0, 149.1, 141.3, 140.2, 132.4, 131.33, 130.9, 126.7, 120.2, 119.1, 114.3, 110.5, 90.9, 85.8, 83.9, 83.3, 56.8, 56.0, 54.3, 28.5, 27.8, 27.1, 25.4, 24.3. HRMS (ESI): calculated for $C_{32}H_{43}N_8O_5$ $[M+H]^+$ 619.3356, found 619.3358.

4-((*E*)-3-((((3*aR*,4*R*,6*R*,6*aR*)-6-(6-amino-9*H*-purin-9-yl)-2,2-dimethyltetrahydrofuro[3,4-*d*][1,3]dioxol-4-yl)methyl)(2-aminoethyl)amino)prop-1-en-1-yl)benzonitrile (**15a**). To a solution of **14a** (118 mg, 0.2 mmol) in CH_2Cl_2 (9 mL) was added TFA (1 mL), after 1 hour, solvent and TFA were removed under reduced pressure, the crude yellow oil was used for next step directly

without purification (assumed quantitative yield). LRMS (ESI): calculated for C₂₅H₃₁N₈O₃ [M+H]⁺ 491.25, found 491.27.

4-((*E*)-3-((((3*aR*,4*R*,6*R*,6*aR*)-6-(6-amino-9*H*-purin-9-yl)-2,2-dimethyltetrahydrofuro[3,4-*d*][1,3]dioxol-4-yl)methyl)(3-aminopropyl)amino)prop-1-en-1-yl)benzonitrile (**15b**). Following the procedure described for compound **15a**, compound **14b** was selectively deprotected, the crude compound **6b** was used for next step directly without purification (assumed quantitative yield). LRMS (ESI): calculated for C₂₆H₃₃N₈O₃ [M+H]⁺ 505.26, found 505.31.

4-((*E*)-3-((((3*aR*,4*R*,6*R*,6*aR*)-6-(6-amino-9*H*-purin-9-yl)-2,2-dimethyltetrahydrofuro[3,4-*d*][1,3]dioxol-4-yl)methyl)(3-aminopropyl)amino)prop-1-en-1-yl)benzonitrile (**15c**). Following the procedure described for compound **15a**, compound **14c** was selectively deprotected, the crude compound **6c** was used for next step directly without purification (assumed quantitative yield). LRMS (ESI): calculated for C₂₇H₃₅N₈O₃ [M+H]⁺ 519.28, found 519.33.

N-(2-((((3*aR*,4*R*,6*R*,6*aR*)-6-(6-amino-9*H*-purin-9-yl)-2,2-dimethyltetrahydrofuro[3,4-*d*][1,3]dioxol-4-yl)methyl)((*E*)-3-(4-cyanophenyl)allyl)amino)ethyl)acrylamide (**16a**). Following the procedure described for compound **11a**, compound **15a** (25 mg, 0.05 mmol) and acryloyl chloride (0.05 mL) afforded compound **7a** as yellow oil without purification for next step.

N-(2-((((3*aR*,4*R*,6*R*,6*aR*)-6-(6-amino-9*H*-purin-9-yl)-2,2-dimethyltetrahydrofuro[3,4-*d*][1,3]dioxol-4-yl)methyl)((*E*)-3-(4-cyanophenyl)allyl)amino)ethyl)-2-chloroacetamide (**16b**). Following the procedure described for compound **11a**, compound **15a** (25 mg, 0.05 mmol) and 2-chloroacetyl chloride (0.05 mL) afforded compound **16b** as yellow oil without purification for next step.

N-(3-((((3*aR*,4*R*,6*R*,6*aR*)-6-(6-amino-9*H*-purin-9-yl)-2,2-dimethyltetrahydrofuro[3,4-*d*][1,3]dioxol-4-yl)methyl)((*E*)-3-(4-cyanophenyl)allyl)amino)propyl)acrylamide. (**16c**) Following the procedure described for compound **11a**, compound **15b** (25 mg, 0.05 mmol) and acryloyl chloride (0.05 mL) afforded compound **16c** as yellow oil without purification for next step.

N-(3-((((3*aR*,4*R*,6*R*,6*aR*)-6-(6-amino-9*H*-purin-9-yl)-2,2-dimethyltetrahydrofuro[3,4-*d*][1,3]dioxol-4-yl)methyl)((*E*)-3-(4-cyanophenyl)allyl)amino)propyl)-2-chloroacetamide (**16d**).

Following the procedure described for compound **11a**, compound **15b** (25 mg, 0.05 mmol) and 2-chloroacetyl chloride (0.05 mL) afforded compound **16d** as yellow oil without purification for next step.

N-(4-(((3*aR*,4*R*,6*R*,6*aR*)-6-(6-amino-9*H*-purin-9-yl)-2,2-dimethyltetrahydrofuro[3,4-*d*][1,3]dioxol-4-yl)methyl)((*E*)-3-(4-cyanophenyl)allyl)amino)butyl)acrylamide (**16e**). Following the procedure described for compound **11a**, compound **15c** (26 mg, 0.05 mmol) and acryloyl chloride (0.05 mL) afforded compound **16e** as yellow oil without purification for next step.

N-(4-(((3*aR*,4*R*,6*R*,6*aR*)-6-(6-amino-9*H*-purin-9-yl)-2,2-dimethyltetrahydrofuro[3,4-*d*][1,3]dioxol-4-yl)methyl)((*E*)-3-(4-cyanophenyl)allyl)amino)butyl)-2-chloroacetamide (**16f**). Following the procedure described for compound **11a**, compound **15c** (26 mg, 0.05 mmol) and 2-chloroacetyl chloride (0.05 mL) afforded compound **16f** as yellow oil without purification for next step.

N-(2-(((2*R*,3*S*,4*R*,5*R*)-5-(6-amino-9*H*-purin-9-yl)-3,4-dihydroxytetrahydrofuran-2-yl)methyl)((*E*)-3-(4-cyanophenyl)allyl)amino)ethyl)acrylamide (**17a**). Following the procedure described for compound **12a**, compound **16a** was deprotected and purified, affording compound **17a** as a yellow powder (3 mg, 18% yield over two steps). ¹H NMR (500 MHz, CD₃OD) δ 8.39 (s, 1H), 8.30 (s, 1H), 7.72 (d, *J* = 8.4 Hz, 2H), 7.56 (d, *J* = 8.3 Hz, 2H), 6.93 (br d, *J* = 15.8 Hz, 1H), 6.54 – 6.45 (m, 1H), 6.16 – 6.03 (m, 3H), 5.65 (dd, *J* = 9.6, 2.2 Hz, 1H), 4.80 (d, *J* = 3.7 Hz, 1H), 4.56 (d, *J* = 10.5 Hz, 1H), 4.49 (t, *J* = 4.9 Hz, 1H), 4.23 (d, *J* = 7.2 Hz, 2H), 3.96 – 3.87 (m, 1H), 3.73 (d, *J* = 3.9 Hz, 1H), 3.70 (d, *J* = 2.3 Hz, 1H), 3.67 (d, *J* = 9.4 Hz, 1H), 3.55 – 3.44 (m, 2H). ¹³C NMR (126 MHz, CD₃OD) δ 168.6, 139.7, 139.1, 132.4, 129.3, 127.4, 126.8, 119.7, 118.1, 112.0, 90.9, 78.7, 73.8, 73.2, 55.1, 34.9, HRMS (ESI): calculated for C₂₅H₂₉N₈O₄ [M+H]⁺ 505.2312, found 505.2218.

N-(2-(((2*R*,3*S*,4*R*,5*R*)-5-(6-amino-9*H*-purin-9-yl)-3,4-dihydroxytetrahydrofuran-2-yl)methyl)((*E*)-3-(4-cyanophenyl)allyl)amino)ethyl)-2-chloroacetamide (**17b**). Following the procedure described for compound **12a**, compound **16b** was deprotected and purified, affording compound **17b** as a yellow powder (12 mg, 38% yield over two steps). ¹H NMR (500 MHz, CD₃OD) δ 8.49 (s, 1H), 8.36 (s, 1H), 7.68 (d, *J* = 8.4 Hz, 2H), 7.52 (d, *J* = 8.3 Hz, 2H), 6.86 (d, *J* = 15.8 Hz, 1H), 6.50 (dd, *J* = 15.4, 7.9 Hz, 1H), 6.17 (d, *J* = 3.8 Hz, 1H), 4.74 – 4.70 (m, 1H), 4.59 – 4.52 (m, 2H), 4.06 (s, 2H), 3.90 (dd, *J* = 13.9, 9.9 Hz, 1H), 3.76 (dd, *J* = 13.9, 1.6 Hz, 1H), 3.69 (t, *J* = 6.1 Hz, 2H), 3.51 (t, *J* = 6.1 Hz, 2H). ¹³C NMR (126 MHz, CD₃OD) δ 169.5,

151.1, 148.2, 139.8, 138.9, 132.4, 127.3, 120.0, 119.9, 118.2, 111.9, 91.1, 78.7, 73.5, 72.3, 55.6, 54.94, 54.9, 52.9, 41.7, 34.8, HRMS (ESI): calculated for C₂₄H₂₇ClN₈O₄ [M+H]⁺ 527.1922, found 527.1925.

***N*-(3-((((2*R*,3*S*,4*R*,5*R*)-5-(6-amino-9*H*-purin-9-yl)-3,4-dihydroxytetrahydrofuran-2-yl)methyl)((*E*)-3-(4-cyanophenyl)allyl)amino)propyl)acrylamide (17c).** Following the procedure described for compound **12a**, compound **16c** was deprotected and purified, affording compound **17c** as a yellow powder (14mg, 44% yield over two steps, > 70% pure). LRMS (ESI): calculated for C₂₆H₃₁N₈O₄ [M+H]⁺ 519.24, found 519.29.

***N*-(3-((((2*R*,3*S*,4*R*,5*R*)-5-(6-amino-9*H*-purin-9-yl)-3,4-dihydroxytetrahydrofuran-2-yl)methyl)((*E*)-3-(4-cyanophenyl)allyl)amino)propyl)-2-chloroacetamide (17d).** Following the procedure described for compound **12a**, compound **16d** was deprotected and purified, affording compound **17d** as a yellow powder (14 mg, 42% yield over two steps). ¹H NMR (500 MHz, CD₃OD) δ 8.48 (s, 1H), 8.35 (s, 1H), 7.68 (d, *J* = 8.2 Hz, 2H), 7.52 (d, *J* = 7.0 Hz, 2H), 6.87 – 6.80 (m, 1H), 6.48 – 6.42 (m, 1H), 6.17 (d, *J* = 3.4 Hz, 1H), 4.68 (s, 1H), 4.56 – 4.51 (m, 2H), 4.12 (d, *J* = 7.3 Hz, 2H), 4.02 (s, 2H), 3.86 – 3.81 (m, 1H), 3.68 (br d, *J* = 13.6 Hz, 1H), 3.38 – 3.33 (m, 2H), 2.06 – 2.01 (m, 2H). ¹³C NMR (126 MHz, CD₃OD) δ 168.7, 161.3, 161.0, 151.1, 148.2, 139.7, 138.6, 132.4, 127.3, 120.0, 119.8, 118.1, 111.9, 90.5, 55.27, 73.5, 72.3, 55.3, 51.3, 41.8, 36.3, 23.9, HRMS (ESI): calculated for C₂₅H₃₀ClN₈O₄ [M+H]⁺ 541.2079, found 541.2083.

***N*-(4-((((2*R*,3*S*,4*R*,5*R*)-5-(6-amino-9*H*-purin-9-yl)-3,4-dihydroxytetrahydrofuran-2-yl)methyl)((*E*)-3-(4-cyanophenyl)allyl)amino)butyl)acrylamide (17e).** Following the procedure described for compound **12a**, compound **16e** was deprotected and purified, affording compound **17e** as a yellow powder (12mg, 36% yield over two steps, >70% pure). LRMS (ESI): calculated for C₂₇H₃₃ClN₈O₄ [M+H]⁺ 533.26, found 533.30.

***N*-(4-((((2*R*,3*S*,4*R*,5*R*)-5-(6-amino-9*H*-purin-9-yl)-3,4-dihydroxytetrahydrofuran-2-yl)methyl)((*E*)-3-(4-cyanophenyl)allyl)amino)butyl)-2-chloroacetamide (17f).** Following the procedure described for compound **12f**, compound **16f** was deprotected and purified, affording compound **17f** as a yellow powder (16 mg, 47% yield over two steps). ¹H NMR (500 MHz, CD₃OD) δ 8.47 (s, 1H), 8.34 (s, 1H), 7.68 (d, *J* = 8.0 Hz, 2H), 7.49 (s, 2H), 6.81 (br d, *J* = 15.8 Hz, 1H), 6.48 – 6.42 (m, 1H), 6.17 (d, *J* = 3.3 Hz, 1H), 4.68 (s, 1H), 4.56 – 4.50 (m, 2H), 4.10

(d, $J = 7.3$ Hz, 2H), 4.06 (s, 2H), 3.84 – 3.79 (m, 1H), 3.66 (br d, $J = 13.4$ Hz, 1H), 3.39 – 3.33 (m, 2H), 3.27 (t, $J = 6.5$ Hz, 2H), 1.89 – 1.75 (m, 2H), 1.65 – 1.56 (m, 2H). ^{13}C NMR (126 MHz, CD_3OD) δ 168.3, 161.1, 151.3, 148.11, 139.7, 138.6, 132.4, 119.8, 118.1, 111.9, 91.2, 73.5, 72.3, 53.4, 41.9, 38.2, 26.1, 20.9, HRMS (ESI): calculated for $\text{C}_{26}\text{H}_{32}\text{ClN}_8\text{O}_4$ $[\text{M}+\text{H}]^+$ 555.2235, found 555.2238.

tert-butyl 3-((((3*aR*,4*R*,6*R*,6*aR*)-6-(6-amino-9*H*-purin-9-yl)-2,2-dimethyltetrahydrofuro[3,4-*d*][1,3]dioxol-4-yl)methyl)((*E*)-3-(4-cyanophenyl)allyl)amino)azetidine-1-carboxylate (**19a**). Following the procedure described for compound **14a**, compound **1b** (40 mg, 0.090 mmol) coupled with *tert*-butyl 3-oxoazetidine-1-carboxylate **18a** (19 mg, 0.11 mmol) afforded compound **19a** as yellow powder (10 mg 19% yield over two steps, > 70% pure). LRMS (ESI): calculated for $\text{C}_{31}\text{H}_{39}\text{N}_8\text{O}_5$ $[\text{M}+\text{H}]^+$ 603.30, found 603.31.

tert-butyl 3-((((3*aR*,4*R*,6*R*,6*aR*)-6-(6-amino-9*H*-purin-9-yl)-2,2-dimethyltetrahydrofuro[3,4-*d*][1,3]dioxol-4-yl)methyl)((*E*)-3-(4-cyanophenyl)allyl)amino)pyrrolidine-1-carboxylate (**19b**). Following the procedure described for compound **14a**, compound **1b** (200 mg, 0.45 mmol) coupled with *tert*-butyl 3-oxoazetidine-1-carboxylate **18b** (92 mg, 0.54 mmol) afforded compound **19b** as yellow powder (174 mg, 63 yield). ^1H NMR (400 MHz, CDCl_3) δ 8.25 (br d, $J = 34.0$ Hz, 1H), 7.87 (s, 1H), 7.51 – 7.43 (m, 2H), 7.22 (br d, $J = 19.8$ Hz, 2H), 6.78 – 6.67 (m, 2H), 6.42 – 6.32 (m, 1H), 6.29 – 6.18 (m, 1H), 6.03 (d, $J = 2.0$ Hz, 1H), 5.43 – 5.39 (m, 1H), 5.05 – 4.96 (m, 1H), 4.38 – 4.26 (m, 1H), 3.67 – 2.99 (m, 7H), 2.93 – 2.73 (m, 2H), 1.98 – 1.86 (m, 1H), 1.78 – 1.63 (m, 1H), 1.54 (s, 3H), 1.39 (d, $J = 5.5$ Hz, 9H), 1.34 (s, 3H). ^{13}C NMR (101 MHz, CDCl_3) δ 155.9, 154.5, 153.0, 149.0, 140.2, 140.2, 132.4, 130.8, 126.6, 120.3, 119.0, 114.4, 110.6, 90.7, 86.2, 84.0, 83.1, 79.4, 61.9, 60.8, 54.7, 44.7, 44.3, 29.7, 28.5, 27.2, 25.5. HRMS (ESI): calculated for $\text{C}_{32}\text{H}_{41}\text{ClN}_8\text{O}_5$ $[\text{M}+\text{H}]^+$ 617.3200, found 617.3201.

tert-butyl 4-((((3*aR*,4*R*,6*R*,6*aR*)-6-(6-amino-9*H*-purin-9-yl)-2,2-dimethyltetrahydrofuro[3,4-*d*][1,3]dioxol-4-yl)methyl)((*E*)-3-(4-cyanophenyl)allyl)amino)piperidine-1-carboxylate (**19c**). Following the procedure described for compound **14a**, compound **1b** (40 mg, 0.090 mmol) coupled with *tert*-butyl 3-oxoazetidine-1-carboxylate **18c** (22 mg, 0.11 mmol) afforded compound **19c** as yellow powder (13mg, 23% yield). LRMS (ESI): calculated for $\text{C}_{33}\text{H}_{41}\text{N}_8\text{O}_5$ $[\text{M}+\text{H}]^+$ 631.33, found 631.35.

4-((*E*)-3-((1-acryloylazetid-3-yl)((2*R*,3*S*,4*R*,5*R*)-5-(6-amino-9*H*-purin-9-yl)-3,4-dihydroxytetrahydrofuran-2-yl)methyl)amino)prop-1-en-1-yl)benzonitrile (**22a**). To a solution of compound **19a** (30 mg, 0.05 mmol) in CH₂Cl₂ (9 mL) was added TFA (1 mL), after 30 mins, solvent was removed under reduced pressure, the crude oil was redissolved in CH₂Cl₂ (10 mL), DIPEA (0.1 mL) added and acryloyl chloride (0.05 mL) was added under 0 °C. After 2 hours, solvent was removed under reduced pressure. A mixture of TFA/CH₂Cl₂/H₂O (9mL/1mL/1mL) was added to the crude oil, after 2 hours, solvent was removed and the crude compound was purified by prep-HPLC to offer compound **22a** as yellow powder, (9 mg, 29% yield over 3 steps, >70% pure). LRMS (ESI): calculated for C₂₆H₂₉N₈O₄ [M+H]⁺ 517.23, found 517.29.

4-((*E*)-3-(((2*R*,3*S*,4*R*,5*R*)-5-(6-amino-9*H*-purin-9-yl)-3,4-dihydroxytetrahydrofuran-2-yl)methyl)(1-(2-chloroacetyl)azetid-3-yl)amino)prop-1-en-1-yl)benzonitrile (**22b**). Following the procedure described for compound **22a**, compound **22b** was obtained as a white powder (11 mg, 35% yield over 3 steps). ¹H NMR (300 MHz, CD₃OD) δ 8.46 (s, 1H), 8.34 (s, 1H), 7.69 (d, *J* = 8.4 Hz, 2H), 7.51 (d, *J* = 8.2 Hz, 2H), 6.88 – 6.73 (m, 1H), 6.51 – 6.41 (m, 1H), 6.14 (d, *J* = 3.5 Hz, 1H), 4.75 – 4.65 (m, 2H), 4.61 – 4.33 (m, 5H), 4.29 – 4.17 (m, 3H), 4.05 (d, *J* = 4.2 Hz, 2H), 3.93 (d, *J* = 9.9 Hz, 2H), 3.63 – 3.41 (m, 2H), 2.70 (d, *J* = 2.7 Hz, 1H). ¹³C NMR (75 MHz, CD₃OD) δ 167.2, 146.8, 143.7, 131.6, 126.5, 117.0, 88.9, 77.7, 74.1, 71.6, 53.7, 53.5, 52.4, 51.4, 39.6, 21.8. HRMS (ESI): calculated for C₂₅H₂₈ClN₈O₄ [M+H]⁺ 539.1922, found 539.1923.

4-((*E*)-3-((1-acryloylpyrrolidin-3-yl)((2*R*,3*S*,4*R*,5*R*)-5-(6-amino-9*H*-purin-9-yl)-3,4-dihydroxytetrahydrofuran-2-yl)methyl)amino)prop-1-en-1-yl)benzonitrile (**22c**). Following the procedure described for compound **22a**, compound **22c** was obtained as a yellow powder (7mg, 23% yield over 3 steps, >70% pure). LRMS (ESI): calculated for C₂₇H₃₁ClN₈O₄ [M+H]⁺ 531.24, found 531.26.

4-((*E*)-3-(((2*R*,3*S*,4*R*,5*R*)-5-(6-amino-9*H*-purin-9-yl)-3,4-dihydroxytetrahydrofuran-2-yl)methyl)(1-(2-chloroacetyl)pyrrolidin-3-yl)amino)prop-1-en-1-yl)benzonitrile (**22d**). Following the procedure described for compound **22a**, compound **22d** was obtained as a white powder (13 mg, 39% yield, over 3 steps). ¹H NMR (300 MHz, CD₃OD) δ 8.42 (s, 1H), 8.38 – 8.26 (m, 1H), 7.70 – 7.66 (m, 2H), 7.53 – 7.39 (m, 2H), 6.91 – 6.72 (m, 1H), 6.54 – 6.40 (m, 1H), 6.21 – 6.11 (m, 1H), 4.75 – 4.47 (m, 4H), 4.29 – 4.08 (m, 5H), 4.02 – 3.55 (m, 6H), 2.70 – 2.68 (m, 1H), 2.39 – 2.33 (m, 2H). ¹³C NMR (75 MHz, CD₃OD) δ 165.5, 150.9, 148.0, 145.1,

131.6, 125.1, 96.4, 77.5, 72.9, 69.5, 53.5, 52.4, 51.3, 39.3, 24.3, HRMS (ESI): calculated for $C_{26}H_{30}ClN_8O_4$ $[M+H]^+$ 553.2079, found 553.2081.

4-((*E*)-3-((1-acryloylpiperidin-4-yl)(((2*R*,3*S*,4*R*,5*R*)-5-(6-amino-9*H*-purin-9-yl)-3,4-dihydroxytetrahydrofuran-2-yl)methyl)amino)prop-1-en-1-yl)benzonitrile (**22e**). Following the procedure described for compound **22a**, compound **22e** was obtained as a white powder (9 mg, 27% yield over 3 steps). LRMS (ESI): calculated for $C_{26}H_{33}N_8O_4$ $[M+H]^+$ 545.26, found 545.31.

4-((*E*)-3-(((2*R*,3*S*,4*R*,5*R*)-5-(6-amino-9*H*-purin-9-yl)-3,4-dihydroxytetrahydrofuran-2-yl)methyl)(1-(2-chloroacetyl)piperidin-4-yl)amino)prop-1-en-1-yl)benzonitrile (**22f**). Following the procedure described for compound **22a**, compound **22f** was obtained as a white powder (10 mg, 30% yield over 3 steps). 1H NMR (400 MHz, CD_3OD) δ 8.38 (s, 1H), 8.27 (s, 1H), 7.67 (d, J = 7.9 Hz, 2H), 7.44 (s, 2H), 6.83 (br d, J = 15.7 Hz, 1H), 6.49 – 6.40 (m, 1H), 6.14 (d, J = 2.4 Hz, 1H), 4.74 – 4.57 (m, 3H), 4.47 (t, J = 7.4 Hz, 1H), 4.38 – 4.34 (m, 1H), 4.30 – 4.25 (m, 1H), 4.16 (d, J = 7.2 Hz, 3H), 3.90 – 3.72 (m, 3H), 3.30 – 3.15 (m, 1H), 2.82 – 2.72 (m, 1H), 2.23 (d, J = 26.9 Hz, 2H), 1.99 – 1.72 (m, 2H). ^{13}C NMR (101 MHz, CD_3OD) δ 166.1, 148.2, 139.6, 138.0, 131.5, 127.1, 120.9, 119.7, 118.1, 111.9, 91.2, 73.5, 72.2, 52.2, 44.2, 40.6, 29.8. HRMS (ESI): calculated for $C_{27}H_{32}ClN_8O_4$ $[M+H]^+$ 567.2235, found 567.2241.

tert-butyl 3-((((3*aR*,4*R*,6*R*,6*aR*)-6-(6-amino-9*H*-purin-9-yl)-2,2-dimethyltetrahydrofuro[3,4-*d*][1,3]dioxol-4-yl)methyl)((*E*)-3-(4-cyanophenyl)allyl)amino)methyl)azetidine-1-carboxylate (**24**). Following the procedure described for compound **14a**, compound **1b** (40 mg, 0.090 mmol) coupled with *tert*-butyl 3-formylazetidine-1-carboxylate **23** (19 mg, 0.11 mmol) afforded compound **24** as yellow powder (35 mg, 63% yield). LRMS (ESI): calculated for $C_{32}H_{41}N_8O_5$ $[M+H]^+$ 617.32, found 617.33.

4-((*E*)-3-(((1-acryloylazetidin-3-yl)methyl)(((2*R*,3*S*,4*R*,5*R*)-5-(6-amino-9*H*-purin-9-yl)-3,4-dihydroxytetrahydrofuran-2-yl)methyl)amino)prop-1-en-1-yl)benzonitrile (**27a**). Following the procedure described for compound **22a**, compound **27a** was obtained as a yellow powder (6 mg, 20% yield over three steps). LRMS (ESI): calculated for $C_{27}H_{31}N_8O_4$ $[M+H]^+$ 531.24, found 531.28.

4-((*E*)-3-((((2*R*,3*S*,4*R*,5*R*)-5-(6-amino-9*H*-purin-9-yl)-3,4-dihydroxytetrahydrofuran-2-yl)methyl)((1-(2-chloroacetyl)azetidin-3-yl)methyl)amino)prop-1-en-1-yl)benzonitrile (27b).

Following the procedure described for compound 27a, compound 27b was obtained as a white powder (9 mg, 28% yield over three steps). ¹H NMR (400 MHz, CD₃OD) δ 8.47 (s, 1H), 8.33 (s, 1H), 7.69 (d, *J* = 8.4 Hz, 2H), 7.48 (d, *J* = 8.2 Hz, 2H), 6.82 (d, *J* = 15.8 Hz, 1H), 6.51 – 6.44 (m, 1H), 6.18 (d, *J* = 3.2 Hz, 1H), 4.70 – 4.64 (m, 1H), 4.62 – 4.43 (m, 4H), 4.12 (d, *J* = 7.4 Hz, 3H), 4.03 (d, *J* = 6.7 Hz, 2H), 3.91 – 3.77 (m, 2H), 3.74 – 3.67 (m, 3H), 3.31 (d, *J* = 6.8 Hz, 1H). ¹³C NMR (101 MHz, CD₃OD) δ 167.3, 161.6, 151.7, 148.1, 142.9, 139.7, 138.7, 132.3, 127.2, 120.0, 118.1, 111.9, 91.2, 78.5, 73.5, 72.3, 55.8, 54.2, 52.0, 38.8, 29.8, 24.7, HRMS (ESI): calculated for C₂₆H₃₀ClN₈O₄ [M+H]⁺ 553.2079, found 553.2082.

tert-butyl (2-((((((3*aR*,4*R*,6*R*,6*aR*)-6-(6-amino-9*H*-purin-9-yl)-2,2-dimethyltetrahydrofuro[3,4-*d*][1,3]dioxol-4-yl)methyl)((*E*)-3-(4-cyanophenyl)allyl)amino)methyl)phenyl)carbamate (29a). Following the procedure described for compound 14a, compound 1b (200 mg, 0.45 mmol) coupled with *tert*-butyl (2-formylphenyl)carbamate 28a (24 mg, 0.11 mmol) afforded compound 29a as yellow powder (61 mg, 21% yield). LRMS (ESI): calculated for C₃₅H₄₁N₈O₅ [M+H]⁺ 653.32, found 653.35.

tert-butyl (3-((((((3*aR*,4*R*,6*R*,6*aR*)-6-(6-amino-9*H*-purin-9-yl)-2,2-dimethyltetrahydrofuro[3,4-*d*][1,3]dioxol-4-yl)methyl)((*E*)-3-(4-cyanophenyl)allyl)amino)methyl)phenyl)carbamate (29b). Following the procedure described for compound 14a, compound 1b (200 mg, 0.45 mmol) coupled with *tert*-butyl (3-formylphenyl)carbamate 28b (150 mg, 0.67 mmol) afforded compound 29b as yellow powder (110 mg, 38% yield). ¹H NMR (400 MHz, CDCl₃) δ 8.18 (s, 1H), 7.92 (s, 1H), 7.47 (d, *J* = 8.3 Hz, 3H), 7.28 (d, *J* = 8.3 Hz, 2H), 7.22 – 7.09 (m, 2H), 6.90 (d, *J* = 7.4 Hz, 1H), 6.75 (s, 2H), 6.43 (br d, *J* = 15.9 Hz, 1H), 6.34 – 6.25 (m, 1H), 6.07 (d, *J* = 2.2 Hz, 1H), 5.38 (dd, *J* = 6.4, 1.9 Hz, 1H), 4.96 (dd, *J* = 6.3, 3.2 Hz, 1H), 4.43 – 4.39 (m, 1H), 3.58 (br d, *J* = 15.1 Hz, 2H), 3.31 – 3.21 (m, 2H), 2.76 (d, *J* = 6.2 Hz, 2H), 1.56 (s, 3H), 1.47 (s, 9H), 1.35 (s, 3H). ¹³C NMR (101 MHz, CDCl₃) δ 156.0, 153.0, 149.1, 141.4, 139.8, 139.7, 138.8, 132.3, 131.5, 131.0, 126.7, 123.43, 123.4, 120.1, 119.1, 114.3, 90.7, 85.6, 83.9, 83.2, 59.0, 56.5, 55.6, 28.4, 27.2, 25.4. HRMS (ESI): calculated for C₃₅H₄₁N₈O₅ [M+H]⁺ 653.3200, found 653.3202.

tert-butyl (4-((((((3*aR*,4*R*,6*R*,6*aR*)-6-(6-amino-9*H*-purin-9-yl)-2,2-dimethyltetrahydrofuro[3,4-*d*][1,3]dioxol-4-yl)methyl)((*E*)-3-(4-

cyanophenyl)allyl)amino)methyl)phenyl)carbamate (29c). Following the procedure described for compound **1a**, compound **1b** (200 mg, 0.45 mmol) coupled with *tert*-butyl (4-formylphenyl)carbamate **28c** (150 mg, 0.68 mmol) afforded compound **29c** as yellow powder (165 mg, 56% yield). ^1H NMR (400 MHz, CDCl_3) δ 8.16 (s, 1H), 7.88 (s, 1H), 7.50 (d, J = 8.3 Hz, 2H), 7.31 – 7.23 (m, 4H), 7.18 (d, J = 8.5 Hz, 2H), 6.59 (s, 2H), 6.40 (br d, J = 15.9 Hz, 1H), 6.31 – 6.24 (m, 1H), 6.06 (d, J = 1.9 Hz, 1H), 5.38 (dd, J = 6.4, 1.9 Hz, 1H), 4.93 (dd, J = 6.3, 3.4 Hz, 1H), 4.45 – 4.39 (m, 1H), 3.58 (d, J = 4.4 Hz, 2H), 3.34 – 3.17 (m, 2H), 2.76 (d, J = 6.5 Hz, 2H), 1.58 (s, 3H), 1.49 (s, 9H), 1.36 (s, 3H). LRMS (ESI): calculated for $\text{C}_{35}\text{H}_{41}\text{ClN}_8\text{O}_5$ $[\text{M}+\text{H}]^+$ 653.32, found 653.35.

***N*-(2-((((2*R*,3*S*,4*R*,5*R*)-5-(6-amino-9*H*-purin-9-yl)-3,4-dihydroxytetrahydrofuran-2-yl)methyl)((*E*)-3-(4-cyanophenyl)allyl)amino)methyl)phenyl)acrylamide (31a).** Following the procedure described for compound **27a**, compound **31a** was obtained as a yellow powder (7 mg, 22% yield over three steps, > 70% pure). LRMS (ESI): calculated for $\text{C}_{30}\text{H}_{11}\text{N}_8\text{O}_4$ $[\text{M}+\text{H}]^+$ 567.24, found 567.29.

***N*-(2-((((2*R*,3*S*,4*R*,5*R*)-5-(6-amino-9*H*-purin-9-yl)-3,4-dihydroxytetrahydrofuran-2-yl)methyl)((*E*)-3-(4-cyanophenyl)allyl)amino)methyl)phenyl)-2-chloroacetamide (31b).** Following the procedure described for compound **27a**, compound **31b** was deprotected and purified, affording compound **31b** as a yellow powder (9 mg, 26% yield over three steps). ^1H NMR (400 MHz, CD_3OD) δ 8.42 (s, 1H), 8.23 (s, 1H), 7.96 (br d, J = 19.4 Hz, 1H), 7.70 (d, J = 8.1 Hz, 2H), 7.58 – 7.39 (m, 4H), 7.32 (d, J = 7.1 Hz, 1H), 6.87 (br d, J = 15.7 Hz, 1H), 6.55 – 6.48 (m, 1H), 6.18 (d, J = 2.1 Hz, 1H), 4.62 – 4.51 (m, 5H), 4.22 (s, 2H), 4.16 (d, J = 5.8 Hz, 2H), 3.80 (d, J = 5.9 Hz, 1H), 3.68 (br d, J = 13.7 Hz, 1H), 2.79 – 2.68 (m, 1H). ^{13}C NMR (101 MHz, CD_3OD) δ 172.7, 166.3, 151.3, 148.0, 139.7, 130.1, 119.8, 118.1, 111.9, 92.8, 81.2, 73.7, 72.3, 57.6, 55.2, 54.1, 42.6, HRMS (ESI): calculated for $\text{C}_{29}\text{H}_{30}\text{ClN}_8\text{O}_4$ $[\text{M}+\text{H}]^+$ 589.2079, found 589.2086.

***N*-(3-((((2*R*,3*S*,4*R*,5*R*)-5-(6-amino-9*H*-purin-9-yl)-3,4-dihydroxytetrahydrofuran-2-yl)methyl)((*E*)-3-(4-cyanophenyl)allyl)amino)methyl)phenyl)acrylamide (31c).** Following the procedure described for compound **27a**, compound **31c** was obtained as a yellow powder (11 mg, 33% yield over three steps). LRMS (ESI): calculated for $\text{C}_{30}\text{H}_{11}\text{ClN}_8\text{O}_4$ $[\text{M}+\text{H}]^+$ 567.24, found 567.25.

***N*-(3-((((2*R*,3*S*,4*R*,5*R*)-5-(6-amino-9*H*-purin-9-yl)-3,4-dihydroxytetrahydrofuran-2-yl)methyl)((*E*)-3-(4-cyanophenyl)allyl)amino)methyl)phenyl)-2-chloroacetamide (31d).**

Following the procedure described for compound **27a**, compound **30d** was deprotected and purified, affording compound **32d** as a white powder (13 mg, 38% yield over three steps). ¹H NMR (400 MHz, CD₃OD) δ 8.42 (s, 1H), 8.23 (s, 1H), 7.96 (br d, 1H), 7.70 (d, *J* = 8.1 Hz, 2H), 7.58 – 7.39 (m, 4H), 7.32 (d, *J* = 7.1 Hz, 1H), 6.87 (br d, *J* = 15.7 Hz, 1H), 6.55 – 6.48 (m 1H), 6.18 (d, *J* = 2.1 Hz, 1H), 4.62 – 4.51 (m, 5H), 4.22 (s, 2H), 4.16 (d, *J* = 5.8 Hz, 2H), 3.80 (d, *J* = 5.9 Hz, 1H), 3.68 (br d, *J* = 13.7 Hz, 1H), 2.79 – 2.68 (m, 1H). ¹³C NMR (101 MHz, CD₃OD) δ 172.7, 166.3, 151.3, 148.0, 145.0, 143.1, 139.7, 138.8, 130.07, 132.3, 130.9, 130.1, 119.8, 118.1, 111.9, 91.4, 78.5, 73.7, 72.3, 57.6, 55.2, 54.1, 42.6, 22.9, HRMS (ESI): calculated for C₂₉H₃₀ClN₈O₄ [M+H]⁺ 589.2079, found 589.2088.

***N*-(3-((((2*R*,3*S*,4*R*,5*R*)-5-(6-amino-9*H*-purin-9-yl)-3,4-dihydroxytetrahydrofuran-2-yl)methyl)((*E*)-3-(4-cyanophenyl)allyl)amino)methyl)phenyl)acrylamide (32e).** Following the procedure described for compound **27a**, compound **32e** was obtained as a yellow powder (14 mg, 41% yield over three steps, > 70% pure). LRMS (ESI): calculated for C₃₀H₁₁N₈O₄ [M+H]⁺ 567.24, found 567.24.

***N*-(3-((((2*R*,3*S*,4*R*,5*R*)-5-(6-amino-9*H*-purin-9-yl)-3,4-dihydroxytetrahydrofuran-2-yl)methyl)((*E*)-3-(4-cyanophenyl)allyl)amino)methyl)phenyl)-2-chloroacetamide (32f).**

Following the procedure described for compound **27a**, compound **30f** was deprotected and purified, affording compound **32f** as a yellow powder (13 mg, 37% yield over three steps). ¹H NMR (400 MHz, CD₃OD) δ 8.40 (s, 1H), 8.22 (s, 1H), 7.69 (t, *J* = 8.9 Hz, 4H), 7.50 (t, *J* = 8.3 Hz, 4H), 6.81 (br d, *J* = 15.7 Hz, 1H), 6.51 – 6.45 (m, 1H), 6.16 (s, 1H), 4.55 (br d, *J* = 26.4 Hz, 5H), 4.23 (s, 2H), 4.14 (d, *J* = 13.7 Hz, 2H), 3.86 – 3.73 (m, 1H), 3.65 (br d, *J* = 13.9 Hz, 1H). ¹³C NMR (101 MHz, CD₃OD) δ 166.3, 148.0, 139.9, 139.7, 125.0, 119.8, 118.1, 111.9, 91.5, 73.6, 72.3, 57.4, 55.3, 42.7. HRMS (ESI): calculated for C₂₉H₃₀ClN₈O₄ [M+H]⁺ 589.2079, found 589.2085.

(*E*)-3-(3-oxoprop-1-en-1-yl)benzenesulfonyl fluoride (36a). To a solution of 3-formylbenzenesulfonyl fluoride **35a** (18 mg, 0.1 mmol), in toluene (10 mL) was added (triphenylphosphoranylidene)acetaldehyde (45 mg, 0.15 mmol), the resulting mixture refluxed overnight. The solvent was removed under reduced pressure, the residue was purified by FCC to give **36a** as yellow powder (9 mg, 44% yield). ¹H NMR (400 MHz, CDCl₃) δ 9.73 (d, *J* = 7.5 Hz,

1H), 7.78 (s, 1H), 7.74 (d, $J = 7.8$ Hz, 1H), 7.67 (d, $J = 7.6$ Hz, 1H), 7.56 (t, $J = 7.8$ Hz, 1H), 7.49 (br d, $J = 16.0$ Hz, 1H), 6.75 (dd, $J = 16.0, 7.5$ Hz, 1H).

(*E*)-4-(3-oxoprop-1-en-1-yl)benzenesulfonyl fluoride (36b). Following the procedure described for compound **36a**, 4-formylbenzenesulfonyl fluoride **35b** (250 mg, 1.3 mmol) coupled with (triphenylphosphoranylidene)acetaldehyde (525 mg, 1.73 mmol), compound **36b** was obtained as yellow powder (190 mg, 67% yield). ^1H NMR (500 MHz, CDCl_3) δ 9.81 (s, 1H), 8.12 – 8.05 (m, 2H), 7.82 (d, $J = 9.1$ Hz, 2H), 7.55 (br d, $J = 16.1$ Hz, 1H), 6.89 – 6.81 (m, 1H).

tert-butyl (S)-4-((((3*aR*,4*R*,6*R*,6*aR*)-6-(6-amino-9*H*-purin-9-yl)-2,2-dimethyltetrahydrofuro[3,4-*d*][1,3]dioxol-4-yl)methyl)((*E*)-3-(3-(fluorosulfonyl)phenyl)allyl)amino)-2-((*tert*-butoxycarbonyl)amino)butanoate (**38a**). Following the procedure described for compound **5a**, compound **36a** (13 mg, 0.06 mmol) coupled with *tert*-butyl (S)-4-((((3*aR*,4*R*,6*R*,6*aR*)-6-(6-amino-9*H*-purin-9-yl)-2,2-dimethyltetrahydrofuro[3,4-*d*][1,3]dioxol-4-yl)methyl)amino)-2-((*tert*-butoxycarbonyl)amino)butanoate **37** (28 mg, 0.05 mmol) afforded compound **38a** as white powder (25 mg, 67% yield). ^1H NMR (500 MHz, CDCl_3) δ 8.25 (s, 1H), 7.90 (s, 1H), 7.53 (s, 1H), 7.44 (d, $J = 7.7$ Hz, 2H), 7.39 – 7.35 (m, 1H), 6.42 (d, $J = 15.9$ Hz, 1H), 6.28 – 6.21 (m, 1H), 6.06 (br d, $J = 24.3$ Hz, 2H), 5.61 (d, $J = 8.0$ Hz, 1H), 5.44 (d, $J = 5.5$ Hz, 1H), 4.98 (s, 1H), 4.37 (s, 1H), 4.23 – 4.16 (m, 1H), 3.33 – 3.30 (m, 1H), 3.27 – 3.18 (m, 1H), 2.84 – 2.81 (m, 1H), 2.67 – 2.62 (m, 2H), 2.56 – 2.51 (m, 1H), 2.01 – 1.94 (m, 1H), 1.79 – 1.74 (m, 1H), 1.59 (s, 3H), 1.45 – 1.32 (m, 21H). ^{13}C NMR (125 MHz, CDCl_3) δ 171.7, 155.7, 155.5, 153.1, 149.2, 140.0, 131.4, 131.0, 130.8, 129.4, 129.0, 125.0, 124.0, 122.9, 120.3, 114.5, 90.7, 85.6, 83.9, 83.3, 81.7, 56.9, 56.0, 52.8, 50.7, 29.6, 28.3, 27.9, 27.2, 25.4, HRMS (ESI): calculated for $\text{C}_{35}\text{H}_{49}\text{FN}_7\text{O}_9\text{S}$ $[\text{M}+\text{H}]^+$ 762.3297, found 762.3301.

tert-butyl (S)-4-((((3*aR*,4*R*,6*R*,6*aR*)-6-(6-amino-9*H*-purin-9-yl)-2,2-dimethyltetrahydrofuro[3,4-*d*][1,3]dioxol-4-yl)methyl)((*E*)-3-(4-(fluorosulfonyl)phenyl)allyl)amino)-2-((*tert*-butoxycarbonyl)amino)butanoate (**38b**). Following the procedure described for compound **5a**, compound **36b** (24 mg, 0.12 mmol) **37** (56 mg, 0.1 mmol) afforded compound **38b** as white powder (27 mg, 71%). ^1H NMR (400 MHz, CDCl_3) δ 8.24 (s, 1H), 7.89 (d, $J = 1.8$ Hz, 1H), 7.59 (d, $J = 8.3$ Hz, 2H), 7.43 (d, $J = 8.4$ Hz, 2H), 6.74 (br d, $J = 16.0$ Hz, 1H), 6.62 – 6.56 (m, 1H), 6.48 – 6.32 (m, 2H), 6.13 (br s, 2H), 6.07 (s, 1H), 5.59 (d, $J = 8.2$ Hz, 1H), 5.47 – 5.43 (m, 1H), 5.02 – 5.00 (m, 1H), 4.42 (dd, $J = 4.8, 1.7$ Hz, 2H), 4.26 – 4.21 (m, 1H), 3.37 – 3.25 (m, 2H), 2.87 – 2.80 (m, 2H), 2.71 – 2.52 (m, 3H), 2.07

– 1.90 (m, 1H), 1.81 – 1.76 (m, 1H), 1.62 (s, 3H), 1.48 – 1.32 (m, 21H). ^{13}C NMR (101 MHz, CDCl_3) δ 171.7, 155.6, 153.0149.1, 144.4, 140.1, 134.7, 128.9, 127.7, 127.04, 90.8, 85.7, 84.0, 83.3, 56.2, 52.8, 28.4, 25.5, HRMS (ESI): calculated for $\text{C}_{35}\text{H}_{49}\text{FN}_7\text{O}_9\text{S}$ $[\text{M}+\text{H}]^+$ 762.3297, found 762.3303.

(S)-2-amino-4((((2R,3S,4R,5R)-5-(6-amino-9H-purin-9-yl)-3,4-dihydroxytetrahydrofuran-2-yl)methyl)((E)-3-(3-(fluorosulfonyl)phenyl)allyl)amino)butanoic acid (39a). Following the procedure described for compound **3a**, compound **38a** (10 mg, 0.013 mmol) was deprotected and purified, affording compound **39a** as a white powder (7 mg, 83%). ^1H NMR (400 MHz, CD_3OD) δ 8.50 (s, 1H), 8.29 (s, 1H), 7.68 (s, 1H), 7.64 – 7.60 (m, 2H), 7.53 (t, $J = 7.7$ Hz, 1H), 6.90 (br d, $J = 15.8$ Hz, 1H), 6.49 – 6.42 (m, 1H), 6.17 (d, $J = 4.0$ Hz, 1H), 4.71 – 4.67 (m, 1H), 4.61 – 4.55 (m, 1H), 4.49 (t, $J = 5.4$ Hz, 1H), 4.14 – 4.09 (m, 3H), 3.87 – 3.80 (m, 1H), 3.71 (br d, $J = 13.8$ Hz, 1H), 3.64 – 3.55 (m, 2H), 2.54 – 2.48 (m, 1H), 2.36 – 2.26 (m, 1H). ^{13}C NMR (101 MHz, CD_3OD) δ 170.6, 161.7, 161.3, 161.0, 151.2, 144.9, 143.0, 139.2, 136.3, 131.0, 130.7, 129.4, 125.1, 119.5, 118.0, 115.1, 90.6, 78.9, 73.6, 72.2, 54.8, 51.2, 50.9, 24.9, HRMS (ESI): calculated for $\text{C}_{23}\text{H}_{29}\text{FN}_7\text{O}_7\text{S}$ $[\text{M}+\text{H}]^+$ 566.1833, found 566.1837.

(S)-2-amino-4((((2R,3S,4R,5R)-5-(6-amino-9H-purin-9-yl)-3,4-dihydroxytetrahydrofuran-2-yl)methyl)((E)-3-(4-(fluorosulfonyl)phenyl)allyl)amino)butanoic acid (39b). Following the procedure described for compound **3a**, compound **38b** (10 mg, 0.013 mmol) was deprotected and purified, affording compound **39b** as a white powder (6 mg, 72%). ^1H NMR (500 MHz, CD_3OD) δ 8.47 (s, 1H), 8.34 (s, 1H), 8.01 (d, $J = 8.6$ Hz, 2H), 7.70 (d, $J = 8.5$ Hz, 2H), 6.93 (br d, $J = 15.8$ Hz, 1H), 6.65 – 6.56 (m, 1H), 6.17 (d, $J = 3.8$ Hz, 1H), 4.70 – (m, 1H), 4.59 – 4.54 (m, 1H), 4.53 – 4.50 (m, 1H), 4.15 (h, $J = 7.6$ Hz, 2H), 4.08 (dd, $J = 8.5, 4.6$ Hz, 1H), 3.85 – 3.80 (m, 1H), 3.71 (dd, $J = 13.9, 1.7$ Hz, 1H), 3.66 – 3.53 (m, 2H), 2.53 – 2.46 (m, 1H), 2.31 – 2.27 (m, 1H). ^{13}C NMR (126 MHz, CD_3OD) δ 170.5, 151.6, 142.8, 137.8, 132.2, 122.1, 119.6, 117.7, 115.4, 113.1, 90.8, 79.0, 73.5, 72.5, 55.0, 25.0, HRMS (ESI): calculated for $\text{C}_{23}\text{H}_{29}\text{FN}_7\text{O}_7\text{S}$ $[\text{M}+\text{H}]^+$ 566.1833, found 566.1835.

(E)-3-(3-(4,4,5,5-tetramethyl-1,3,2-dioxaborolan-2-yl)phenyl)acrylaldehyde (41a). Following the procedure described for compound **36a**, compound 3-(4,4,5,5-tetramethyl-1,3,2-dioxaborolan-2-yl)benzaldehyde **40a** (46 mg, 0.2 mmol) coupled with

(triphenylphosphoranylidene)acetaldehyde (90 mg, 0.3 mmol) to offer **41a** as yellow powder (26 mg, 50%). The compound was not stable on silica column and directly used in the next step.

(*E*)-3-(3-(4,4,5,5-tetramethyl-1,3,2-dioxaborolan-2-yl)phenyl)acrylaldehyde (41b).

Following the procedure described for compound **36a**, compound 3-(4,4,5,5-tetramethyl-1,3,2-dioxaborolan-2-yl)benzaldehyde **40b** (46 mg, 0.2 mmol) coupled with (triphenylphosphoranylidene)acetaldehyde (90 mg, 0.3 mmol) to offer **41b** as yellow powder (23 mg, 45%). The compound was not stable on silica column and directly used in the next step.

***tert*-butyl (S)-4-((((3*aR*,4*R*,6*R*,6*aR*)-6-(6-amino-9*H*-purin-9-yl)-2,2-dimethyltetrahydrofuro[3,4-*d*][1,3]dioxol-4-yl)methyl)((*E*)-3-(3-(4,4,5,5-tetramethyl-1,3,2-dioxaborolan-2-yl)phenyl)allyl)amino)-2-((*tert*-butoxycarbonyl)amino)butanoate (42a).**

Following the procedure described for compound **5a**, compound **37** (28 mg, 0.05 mmol) coupled with **41a** (26 mg, 0.10 mmol) afforded compound **42a** as yellow powder (16mg, 39%). The compound was not stable on silica column and directly used in the next step. LRMS (ESI): calculated for C₄₁H₆₁BN₇O₉ [M+H]⁺ 806.46, found 806.50.

***tert*-butyl (S)-4-((((3*aR*,4*R*,6*R*,6*aR*)-6-(6-amino-9*H*-purin-9-yl)-2,2-dimethyltetrahydrofuro[3,4-*d*][1,3]dioxol-4-yl)methyl)((*E*)-3-(4-(4,4,5,5-tetramethyl-1,3,2-dioxaborolan-2-yl)phenyl)allyl)amino)-2-((*tert*-butoxycarbonyl)amino)butanoate (42b).**

Following the procedure described for compound **5a**, compound **37** (28 mg, 0.05 mmol) coupled with **41b** (26 mg, 0.10 mmol) afforded compound **42b** as yellow powder (6 mg, 15%). The compound was not stable on silica column and directly used in the next step. LRMS (ESI): calculated for C₄₁H₆₁BN₇O₉ [M+H]⁺ 806.46, found 806.53.

(S)-2-amino-4-(((2*R*,3*S*,4*R*,5*R*)-5-(6-amino-9*H*-purin-9-yl)-3,4-dihydroxytetrahydrofuran-2-yl)methyl)((*E*)-3-(3-boronophenyl)allyl)amino)butanoic acid (44a).

To a solution of **42a** (40 mg, 0.05mmol) in THF/H₂O = 6 mL/2mL added NaIO₄ (31 mg, 0.15 mmol). The resulting mixture stirred at r.t 30 mins. 0.5 mL 1 M HCl(aq) was added to the solution and stirred 30 mins. The solvent was removed, a mixture of TFA/CH₂Cl₂/H₂O = 9 mL/1mL/1mL was added to the residue, the solution stirred at rt 2h, the solvent was removed, and the crude compound was purified by prep-HPLC to offer final compound **44a** as white powder (12 mg, 38% yield over two steps). ¹H NMR (500 MHz, CD₃OD) δ 8.40 (br, d, *J* = 11.0 Hz, 1H), 8.24 (d, *J* = 7.8 Hz, 1H), 7.70 (br d, *J* = 18.1 Hz, 2H), 7.42 – 7.25 (m, 2H), 6.78 (d, *J* =

16.1 Hz, 1H), 6.31 – 6.25 (m, 1H), 6.14 (d, J = 3.7 Hz, 1H), 4.69 (t, J = 4.2 Hz, 1H), 4.53 (d, J = 2.6 Hz, 2H), 4.14 – 4.00 (m, 2H), 3.99 – 3.94 (m, 1H), 3.86 – 3.76 (m, 1H), 3.70 – 3.48 (m, 4H), 2.49 – 2.39 (m, 1H), 2.20 (d, J = 6.3 Hz, 1H). ^{13}C NMR (126 MHz, CD_3OD) δ 170.8, 141.0, 134.4, 132.0, 127.7, 91.4, 79.1, 73.4, 71.9, 25.2, HRMS (ESI): calculated for $\text{C}_{23}\text{H}_{31}\text{BN}_7\text{O}_7$ $[\text{M}+\text{H}]^+$ 528.2378, found 528.2378.

(*S*)-2-amino-4-((((2*R*,3*S*,4*R*,5*R*)-5-(6-amino-9*H*-purin-9-yl)-3,4-dihydroxytetrahydrofuran-2-yl)methyl)((*E*)-3-(4-boronophenyl)allyl)amino)butanoic acid (44b). Following the procedure described for compound **42a**, compound **42b** (40mg, 0.05 mmol) was deprotected and purified, affording compound **44b** as a white powder (5 mg, 17% yield over two steps). ^1H NMR (500 MHz, CD_3OD) δ 8.43 (s, 1H), 8.26 (s, 1H), 7.69 (s, 2H), 7.30 (d, J = 7.7 Hz, 2H), 6.77 (br d, J = 15.8 Hz, 1H), 6.35 – 6.29 (m, 1H), 6.15 (d, J = 3.6 Hz, 1H), 4.70 (t, J = 4.0 Hz, 1H), 4.54 (d, J = 6.2 Hz, 2H), 4.13 – 3.97 (m, 3H), 3.84 – 3.79 (dd, J = 13.8, 9.9 Hz, 1H), 3.69 – 3.49 (m, 3H), 2.50 – 2.42 (m, 1H), 2.28 – 2.18 (m, 1H). ^{13}C NMR (126 MHz, CD_3OD) δ 148.3, 140.7, 133.9, 125.6, 119.8, 91.0, 79.1, 73.4, 72.4, 54.6, 51.9, 25.1, HRMS (ESI): calculated for $\text{C}_{23}\text{H}_{31}\text{BN}_7\text{O}_7$ $[\text{M}+\text{H}]^+$ 528.2378, found 528.2380.

Modeling protocol by AutoDock Vina

The crystal structure of the human NNMT (6PVS) was retrieved from the Protein Data Bank.³¹ Polar hydrogen atoms were added using AutoDockTools (ADT).³⁰ United atom Kollman charges were assigned for the protein. The 3D structures of the ligands used for the docking studies were constructed using ChemDraw and Chem3D. These ligands were energetically minimized by using Chem3D. The AutoDock vina³⁷ molecular docking program was employed, using a genetic algorithm with local search (GALS). The pose with the highest docking score was exported and analysed by PyMOL 2.4.

References

1. Thomas MG, Sartini D, Emanuelli M, van Haren MJ, Martin NI, Mountford DM, et al. Nicotinamide N-methyltransferase catalyses the N-methylation of the endogenous -carboline norharman: evidence for a novel detoxification pathway. *Biochem J*. 2016;473(19):3253-67.
2. Alston TA, Abeles RH. Substrate specificity of nicotinamide methyltransferase isolated from porcine liver. *Arch Biochem Biophys*. 1988;260(2):601-8.
3. van Haren MJ, Sastre Toraño J, Sartini D, Emanuelli M, Parsons RB, Martin NI. A Rapid and Efficient Assay for the Characterization of Substrates and Inhibitors of Nicotinamide N - Methyltransferase. *Biochemistry*. 2016;55(37):5307-15.
4. Pissios P. Nicotinamide N -Methyltransferase: More Than a Vitamin B3 Clearance Enzyme. *Trends Endocrinol Metab*. 2017;28(5):340-53.
5. Khalil EM, Mackie BD, Mao Y. Methyltransferases: Key Regulators in Cardiovascular Development and Disease. *Ann Vasc Med Res*. 2016;3(2):1032-9.
6. Fedorowicz A, Mateuszuk Ł, Kopec G, Skórka T, Kutryb-Zajac B, Zakrzewska A, et al. Activation of the nicotinamide N-methyltransferase (NNMT)-1-methylnicotinamide (MNA) pathway in pulmonary hypertension. *Respir Res*. 2016;17(1):108.
7. Jung J, Kim LJY, Wang X, Wu Q, Sanvoranart T, Hubert CG, et al. Nicotinamide metabolism regulates glioblastoma stem cell maintenance. *JCI Insight*. 2017;2(10):1-23.
8. Kraus D, Yang Q, Kong D, Banks AS, Zhang L, Rodgers JT, et al. Nicotinamide N-methyltransferase knockdown protects against diet-induced obesity. *Nature*. 2014;508(7495):258-62.
9. ten Klooster JP, Sotiriou A, Boeren S, Vaessen S, Vervoort J, Pieters R. Type 2 diabetes-related proteins derived from an in vitro model of inflamed fat tissue. *Arch Biochem Biophys*. 2018;644(February):81-92.
10. Parsons RB, Smith SW, Waring RH, Williams AC, Ramsden DB. High expression of nicotinamide N -methyltransferase in patients with idiopathic Parkinson ' s disease. *Neurosci Lett*. 2003;342(1-2):13-6.
11. Parsons RB, Smith M-L, Williams AC, Waring RH, Ramsden DB. Expression of Nicotinamide N-Methyltransferase (E.C. 2.1.1.1) in the Parkinsonian Brain. *J Neuropathol Exp Neurol*. 2002;61(2):111-24.
12. Sartini D, Santarelli A, Rossi V, Goteri G, Rubini C, Ciavarella D, et al. Nicotinamide N-Methyltransferase Upregulation Inversely Correlates with Lymph Node Metastasis in Oral Squamous Cell Carcinoma. *Mol Med*. 2007;13(7-8):415-21.

13. Sartini D, Muzzonigro G, Milanese G, Pierella F, Rossi V, Emanuelli M. Identification of Nicotinamide N-Methyltransferase as a Novel Tumor Marker for Renal Clear Cell Carcinoma. *J Urol*. 2006;176(5):2248-54.
14. Zhang J, Wang Y, Li G, Yu H, Xie X. Down-Regulation of Nicotinamide N-methyltransferase Induces Apoptosis in Human Breast Cancer Cells via the Mitochondria-Mediated Pathway. Filleur S, ed. *PLoS One*. 2014;9(2):e89202.
15. Palanichamy K, Kanji S, Gordon N, Thirumoorthy K, Jacob JR, Litzenberg KT, et al. NNMT Silencing Activates Tumor Suppressor PP2A , Inactivates Oncogenic STKs , and Inhibits Tumor Forming Ability. *Cancer Ther Preclin*. 2016;23(9):1-11.
16. Ulanovskaya OA, Zuhl AM, Cravatt BF. NNMT promotes epigenetic remodeling in cancer by creating a metabolic methylation sink. *Nat Chem Biol*. 2013;9(5):300-6.
17. Lim BH, Cho BI, Yu NK, Jae WK, Park ST, Lee CW. Overexpression of nicotinamide N-methyltransferase in gastric cancer tissues and its potential post-translational modification. *Exp Mol Med*. 2006;38(5):455-65.
18. Nemmara V V., Tilwawala R, Salinger AJ, Miller L, Nguyen SH, Weerapana E, et al. Citrullination Inactivates Nicotinamide-N-methyltransferase. *ACS Chem Biol*. 2018;13(9):2663-72.
19. Gao Y, Martin NI, van Haren MJ. Nicotinamide N-methyl transferase (NNMT): An emerging therapeutic target. *Drug Discov Today*. 2021;xxx(xx):1-8.
20. Singh J, Petter RC, Baillie TA, Whitty A. The resurgence of covalent drugs. *Nat Rev Drug Discov*. 2011;10(4):307-17.
21. Peng Y, Sartini D, Pozzi V, Wilk D, Emanuelli M, Yee VC. Structural Basis of Substrate Recognition in Human Nicotinamide N -Methyltransferase. *Biochemistry*. 2011;50(36):7800-8.
22. Horning BD, Suciu RM, Ghadiri DA, Ulanovskaya OA, Matthews ML, Lum KM, et al. Chemical Proteomic Profiling of Human Methyltransferases. *J Am Chem Soc*. 2016;138(40):13335-43.
23. Sen S, Mondal S, Zheng L, Salinger AJ, Fast W, Weerapana E, et al. Development of a Suicide Inhibition-Based Protein Labeling Strategy for Nicotinamide N-Methyltransferase. *ACS Chem Biol*. 2019;14(4):613-8.
24. Lee H-Y, Suciu RM, Horning BD, Vinogradova E V., Ulanovskaya OA, Cravatt BF. Covalent inhibitors of nicotinamide N-methyltransferase (NNMT) provide evidence for target engagement challenges in situ. *Bioorg Med Chem Lett*. 2018;28(16):2682-7.

25. Resnick E, Bradley A, Gan J, Douangamath A, Krojer T, Sethi R, et al. Rapid Covalent-Probe Discovery by Electrophile-Fragment Screening. *J Am Chem Soc.* 2019;141(22):8951-68.
26. Martin JS, MacKenzie CJ, Fletcher D, Gilbert IH. Characterising covalent warhead reactivity. *Bioorg Med Chem.* 2019;27(10):2066-74.
27. Plescica J, Moitessier N. Design and discovery of boronic acid drugs. *Eur J Med Chem.* 2020;195:112270.
28. DAVID E. FAHRN AMG. Sulfonyl Fluorides as Inhibitors of Esterases. I . Rates of Reaction with Acetylcholinesterase, α -Chymo trypsin, and Trypsin. *J Am Chem Soc.* 1963;2016(85):997-1000.
29. Narayanan A, Jones LH. Sulfonyl fluorides as privileged warheads in chemical biology. *Chem Sci.* 2015;6(5):2650-9.
30. Morris GM, Huey R, Lindstrom W, Sanner MF, Belew RK, Goodsell DS, et al. AutoDock4 and AutoDockTools4: Automated docking with selective receptor flexibility. *J Comput Chem.* 2009;30(16):2785-91.
31. Chen D, Li L, Diaz K, Iyamu ID, Yadav R, Noinaj N, et al. Novel Propargyl-Linked Bisubstrate Analogues as Tight-Binding Inhibitors for Nicotinamide N-Methyltransferase. *J Med Chem.* 2019;62(23):10783-97.
32. Dose C, Seitz O. Single nucleotide specific detection of DNA by native chemical ligation of fluorescence labeled PNA-probes. *Bioorganic Med Chem.* 2008;16(1):65-77.
33. Freeman NS, Hurevich M, Gilon C. Synthesis of N-substituted Ddz-protected hydrazines and their application in solid phase synthesis of aza-peptides. *Tetrahedron.* 2009;65(8):1737-45.
34. Zhao T, Kurpiewska K, Kalinowska-Thus^{''} cik J, Herdtweck E, Dömling A. α -Amino Acid-Isosteric α -Amino Tetrazoles. *Chem - A Eur J.* 2016;22(9):3009-18.
35. Han LC, Stanley PA, Wood PJ, Sharma P, Kuruppu AI, Bradshaw TD, et al. Horner-Wadsworth-Emmons approach to piperlongumine analogues with potent anti-cancer activity. *Org Biomol Chem.* 2016;14(31):7585-93.
36. Van Der Zouwen AJ, Lohse J, Wieske LHE, Hohmann KF, Van Der Vlag R, Witte MD. An in situ combinatorial methodology to synthesize and screen chemical probes. *Chem Commun.* 2019;55(14):2050-3.
37. Oleg Trott AJO. Software News and Updates Gabedit — A Graphical User Interface for Computational Chemistry Softwares. *J Comput Chem.* 2010;31(2):455-61.